Confinement Catalysis with 2D Materials for Energy Conversion

Lei Tang, Xianguang Meng, Dehui Deng, and Xinhe Bao*

The unique electronic and structural properties of 2D materials have triggered wide research interest in catalysis. The lattice of 2D materials and the interface between 2D covers and other substrates provide intriguing confinement environments for active sites, which has stimulated a rising area of "confinement catalysis with 2D materials." Fundamental understanding of confinement catalysis with 2D materials will favor the rational design of high-performance 2D nanocatalysts. Confinement catalysis with 2D materials has found extensive applications in energy-related reaction processes, especially in the conversion of small energy-related molecules such as O_2, CH_4, CO, CO_2, H_2O, and CH_3OH. Two representative strategies, i.e., 2D lattice-confined single atoms and 2D cover-confined metals, have been applied to construct 2D confinement catalytic systems with superior catalytic activity and stability. Herein, the recent advances in the design, applications, and structure–performance analysis of two 2D confinement catalytic systems are summarized. The different routes for tuning the electronic states of 2D confinement catalysts are highlighted and perspectives on confinement catalysis with 2D materials toward energy conversion and utilization in the future are provided.

1. Introduction

With the rapid increase of fossil fuels consumption and the continuous growth of global energy demands, the search for renewable energy sources has become a great challenge for sustainable society.[1] Tremendous efforts have been made for the development of energy conversion processes on the basis of the important catalytic systems such as water electrolysis, fuel cells and C1 molecules transformation.[2] The efficiency of these energy conversion systems depend on many factors, but the overall performances strongly rely on the electronic and structural properties of the catalysts. A general catalyst is composed of active center and surrounding environments, in which the former is usually regarded as the dominant function in catalysis but the latter is indispensable to modulate the electronic and geometric structure of active sites. In this respect, confinement catalysis is recognized for its ability to control the structural and electronic properties of active centers at nano or atom precision via the coordination environments.[3] The electronic states of the confined active sites will receive direct influence from their coordination environments, which finally alters the adsorption energetics of catalytic intermediates and consequently changes the catalytic activity and selectivity. For confinement catalysis, one important target is to search the suitable substrates to efficiently confine the active sites, and meanwhile to efficiently stabilize and fully expose the active sites. It needs the substrate materials should have stable structures, novel electronic properties, and highly exposed surface.

Emerging as a novel and promising class of materials, 2D nanomaterials have captured widespread interest and achieved great development over the past two decades.[4] The well-defined structures and unique electronic properties of 2D materials have triggered wide research interest in various catalysis systems, especially in the conversion of small energy-related molecules like the O_2, CO_2, CH_4, CO, H_2O, and CH_3OH,[5] because these small molecules are more sensitive to the electronic properties of the catalytic materials with less structure effect such as steric hindrance compared with the conversion of macromolecules. The lattice of 2D materials and the interface between 2D cover and other active components provide meaningful confining environments for active sites, which has stimulated a new area of "confinement catalysis with 2D materials." Within this lattice- and interface-confined environment, the electronic state of catalytic sites can be easily manipulated to the appropriate values matching the energy level of the substrates, which realizes the feasibility of turning activity. In addition to the precise turning of activity, the unique nanostructure of 2D materials affects kinetic reaction barriers governed by the surroundings of the active site allowing for enhanced selectivity. In addition, the high mechanical strength and thermal stability of 2D materials render it as a promising host for confined active sites. Finally, because of the relatively simple type of catalytic site and the well-defined structure, the atomically thin 2D nanosheets can serve as an ideal model for understanding confinement catalysis. Considering that 2D lattice- and interface-confined catalysts afford a highly active, selective and stable system,

L. Tang, Prof. X. Meng, Prof. D. Deng, Prof. X. Bao
State Key Laboratory of Catalysis
Dalian Institute of Chemical Physics
Chinese Academy of Sciences
Zhongshan Road 457, Dalian 116023, China
E-mail: dhdeng@dicp.ac.cn

L. Tang, Prof. D. Deng, Prof. X. Bao
University of Chinese Academy of Sciences
Beijing 100049, China

The ORCID identification number(s) for the author(s) of this article can be found under https://doi.org/10.1002/adma.201901996.

DOI: 10.1002/adma.201901996

confinement catalysis with 2D materials may be a consummate solution to further improve upon current heterogeneous systems and gain deep understanding of the reaction mechanism.

Based on the confinement catalysis with 2D materials, two types of 2D confinement catalytic systems have been built up including catalysis with 2D lattice-confined single atoms and catalysis with 2D cover-confined metals. The 2D lattice-confined single atoms refer to the single atoms that anchored by or doped in the coordination environment of 2D lattice. It is well-known that the catalytic activity is essentially determined by the electronic states created by the interaction between single atom and the confined coordination environments. 2D materials have unique electronic properties closely depending on the number of layers. When the single atoms, whose electronic states are typically very different from their bulk particles, are confined by 2D materials, new electronic states will be created for potential catalytic processes. In addition, with the advantage of the open structure of 2D materials, the reactants have more opportunities to access the single atom active site anchored by 2D material compared with that of bulk materials. Moreover, a high degree of coordinative unsaturation of the confined single atoms could be maintained in the 2D structure and thus the single atoms in this confining environment generally exhibit unique catalytic performance compared with other types of catalysts. For the catalysts derived from heteroatom doped 2D materials, the catalytic activity of atoms in the vicinity of doped atoms can be induced at the surface of 2D materials. From this aspect, the doped heteroatoms could be used to turn the electronic property and promote catalytic activity of intrinsically inactive 2D nanomaterials. These confined single atoms in ultrathin 2D sheets are advantageous as they maximize the number of reaction sites. Since 2D materials (e.g., graphene) are generally stable and chemically inert, they can provide effective and tight protection for the active metal catalysts against harsh reaction medium. The encapsulation of metals by 2D cover can also protect catalyst against harsh reaction medium such as strong acidity, strong alkalinity, oxidation, poisoning, or sintering. Therefore, this type of catalysts makes it possible to use active but perishable nonprecious metals for potential applications in extreme conditions. It should be of great interest and significance in studying the electronic interaction at the interface between 2D cover and metals. The difference of the work functions between 2D cover and the inner metals will lead to the charge transfer from metal to 2D cover. This will change the work function or electronic states of the outer surface of 2D cover and trigger their catalytic activity for reaction activation. Moreover, the well-defined nanospace between 2D cover and metals offers an ideal microenvironment for exploring the confinement catalysis experimentally and theoretically.

Here, we present recent progress in the confinement catalysis with 2D materials and their wide applications in several important energy-related catalytic processes including water electrolysis, fuel cells, and C1 molecules transformation. Two representative strategies (**Figure 1**), i.e., 2D lattice-confined single atoms and 2D cover-confined metals, will be extensively discussed for constructing 2D confinement catalytic systems. Finally, we will present a brief outlook on future research and development of 2D confinement catalysis for energy conversion.

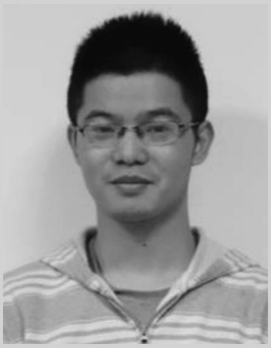

Lei Tang received his B.S. degree from Sichuan University in 2014 and his master's degree from Tianjin University in 2017. He is now pursuing a Ph.D. under the tutelage of Prof. Deng in physical chemistry at Dalian Institute of Chemical Physics (DICP), Chinese Academy of Sciences (CAS). His research interests focus on 2D nanomaterials and hybrid materials for energy-related catalysis.

Dehui Deng received his Ph.D. in physical chemistry from DICP in 2013. He subsequently joined the State Key Laboratory of Catalysis, DICP, as an associate Professor and became a full Professor in 2017. Since January 2015, he has served as an iChEM Professor at Xiamen University. He also served as a visiting scholar at Stanford University between 2015 and 2016. His research interests include fundamental and applied research in heterogeneous catalysis and electrocatalysis, aiming at highly efficient activation and conversion of energy molecules such as O_2, H_2, H_2O, CO, CO_2, CH_4, and CH_3OH.

Xinhe Bao received his Ph.D. in physical chemistry from Fudan University in 1987. He held an Alexander von Humboldt Research Fellow position at the Fritz-Haber Institute, Berlin, between 1989 and 1995. Following that, he joined DICP as a full Professor. He became a member of the CAS in 2009. His research interests are in nano- and interfacial catalysis, focusing on the fundamental understanding of heterogeneous catalysis, including the development of new catalysts and novel catalytic processes related to energy conversion and storage.

2. Catalysis with 2D Lattice-Confined Single Atoms

Single-atom catalysts exhibit unique properties and attract widespread interest for their effectiveness in promoting a variety of

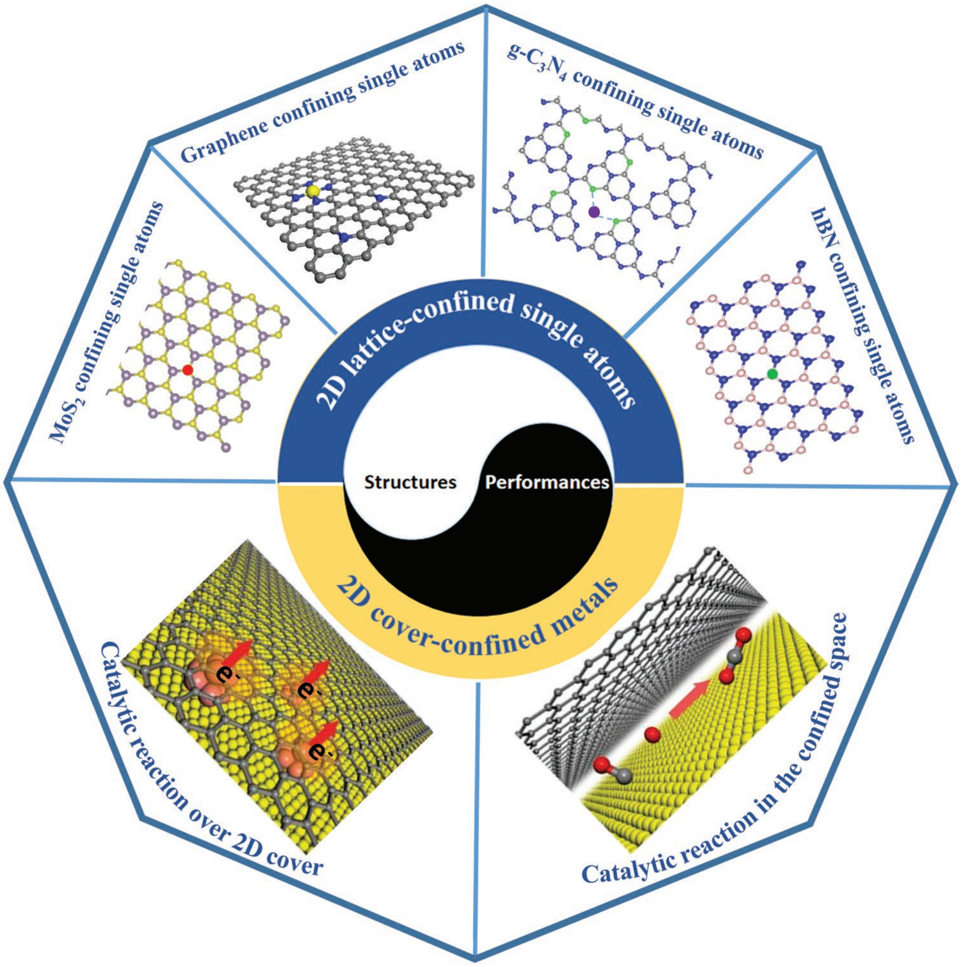

Figure 1. Overview of 2D confinement catalytic systems. Image for "Graphene confining single atoms": Reproduced with permission.[5a] Copyright 2016, Springer Nature. Images for "MoS_2 confining single atoms" and "hBN confining single atoms": Reproduced with permission.[5c] Copyright 2018, American Chemical Society. Image for "Catalytic reaction over 2D cover": Reproduced with permission.[5a] Copyright 2016, Springer Nature. Image for "Catalytic reaction in the confined space": Reproduced with permission.[5a] Copyright 2016, Springer Nature.

catalytic reactions.[6] However, preparation of stable and practical single atoms-based catalysts is still a great challenge, since single atoms have the tendency to aggregate into larger particles under realistic reaction conditions. A strategy to prevent their aggregation, while at the same time maintaining their activity, is to confine them into atomically thin 2D nanosheets. To accomplish this, single-atom catalysts can be stabilized by the lattice of ultrathin 2D nanosheets. Such atomically thin 2D sheets are ideal platforms for four reasons: 1) The single atoms doping into the basal planes of 2D nanosheets can be either directly used as new catalytic sites, or used as heteroatoms to modulate the electronic property of inert 2D nanomaterials and turn the intrinsic activity; 2) Abundant exposed surface atoms within the basal planes of 2D sheets is an advantage as it maximizes the areal density of active site; 3) The unique open structure of 2D nanosheets favors direct identification of the atomic structure information by advanced characterization techniques; and 4) The simple and well-defined 2D nanostructure affords us a suitable model to bridges the theoretical and experimental studies on the structure–performance relationship of nanocatalysts. All these aspects mentioned above demonstrated the experimental and theoretical importance of 2D lattice-confined single atom catalysts in understanding confinement catalysis. In this section, typical 2D nanomaterials (graphene, MoS_2, and g-C_3N_4) confining metal and nonmetal single atom catalysts will be introduced.

2.1. Graphene Confining Single Atoms

2.1.1. Graphene Confining Nonmetal Atoms

Metal-free catalysts are promising substitutes compared with noble-metal-based nanocatalysts for oxygen evolution reaction (OER), hydrogen evolution reaction (HER), oxygen reduction reaction (ORR), and other energy-related catalytic systems because of the low cost. One of the several earliest metal-free nanocatalysts was reported by Dai and co-workers in 2009. In this work, N-doped carbon nanotubes exhibited high catalytic ORR performances which was even comparable with that of

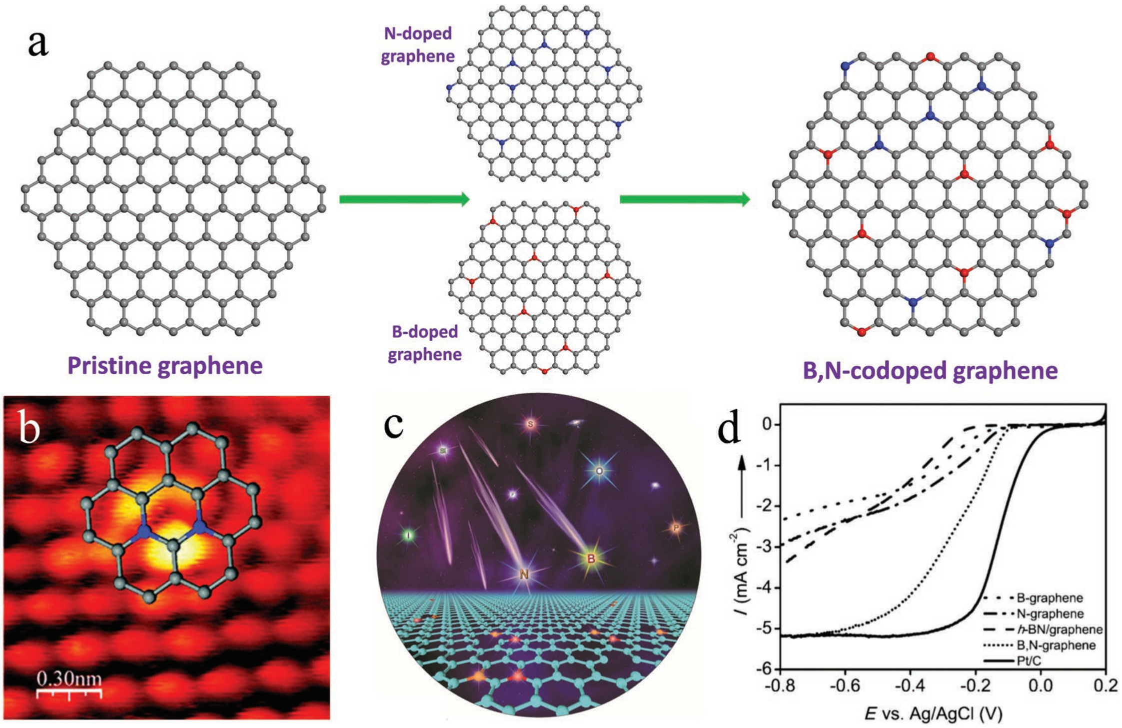

Figure 2. a) The doping configuration of B, N isolated, or B,N-codoped graphene, and the related trend of ORR activity. b) STM images of N-doping graphene. c) A schematic illustration of the B,N-codoped graphene. d) LSV curves for B-doped graphene, N-doped graphene, h-BN/graphene, B,N-codoped graphene, and Pt/C. b) Reproduced with permission.[11] Copyright 2011, American Chemical Society. c,d) Reproduced with permission.[22] Copyright 2013, Wiley-VCH.

precious-metal-based nanocatalysts.[7] Since then, more metal-free catalysts are developed for effective catalytic processes. In particular, heteroatom-doping graphene with highly tunable physicochemical properties have been increasingly reported as typical metal-free nanocatalysts for energy-related catalytic systems.[8] By replacing sp^2 C atoms with N, B, P, S, etc., heteroatom doping leads to polarization in the lattice of graphene because of differences in the electronegativity of atoms, thereby modulating the electronic states and catalytic activity of pristine graphene.[9] Here we will focus on the most recent reports on graphene confining nonmetal atoms (B, N) in the electrocatalysis for ORR (**Figure 2**a).

It has been widely demonstrated that N-doping could enhance the performance of pristine graphene in many energy-related catalytic processes.[10] The introduction of N atoms induced partial positive charge on the neighboring C atoms because of their high electron affinity, which leads to unique electronic properties. One typical example was conducted by Deng et al. in 2011 who synthesized N-doped graphene by a simple method using tetrachloromethane and lithium nitride.[11] The unique electronic structure change manipulated by the N heteroatoms in the lattice was directly confirmed by scanning tunneling microscopy for the first time (Figure 2b). Some N doping forms have been revealed in graphene: oxidized N, iminic N, pyrrolic N, pyridinic N, graphitic N, nitrile N, and amino N.[12] Thus, it is imperative to confirm the active centers of N-doping graphene which are responsible for the ORR. At present, the debate focuses on whether the catalytic sites of N-doping graphene are created by graphitic N or pyridinic N.[13–16] In comparison with the widely reported N-doped graphene, catalysis over graphene confining B atoms is a less studied subject probably because of the difficulties in material synthesis. B element can also lead to the modulation of charge density in the graphene, since the electron-accepting property of B improves O affinity.[17] In general, the enhancement of catalytic performances after B-doping are not as noticeable as those shown in N-doping graphene. In addition, the formation of different B bonding configurations causes difficult to the understanding of the catalytic mechanism in B-doping graphene.[18]

Heteroatoms co-doping has emerged as a promising strategy to further regulate the electronic states, surface structures, and the catalytic performance of graphene-based catalysts. N and B co-doping of graphene has significant enhanced catalytic performance of ORR. Depending on the B, N, and C stoichiometry, two typical heteroatoms co-doping could be synthesized: 1) h-BN domains confined in the lattice of graphene; and 2) N—C and B—C chemical bonding confined in graphene lattice. The synthesis of graphene confining h-BN domains has been studied by Ajayan and co-workers in a CVD process.[19] Previous results demonstrated that the introduction of h-BN domains in the lattice of graphene had limited influenced on the ORR activity due to the inertness of h-BN.[20] Although h-BN domains in the lattice of graphene nanosheet is inactive to ORR, h-BN domains at the zigzag edges showed improved oxygen affinity between C and B.[21] For example, Ajayan and co-workers has prepared graphene nanoribbons confining h-BN domains at the zigzag edges, which exhibited high-performances in

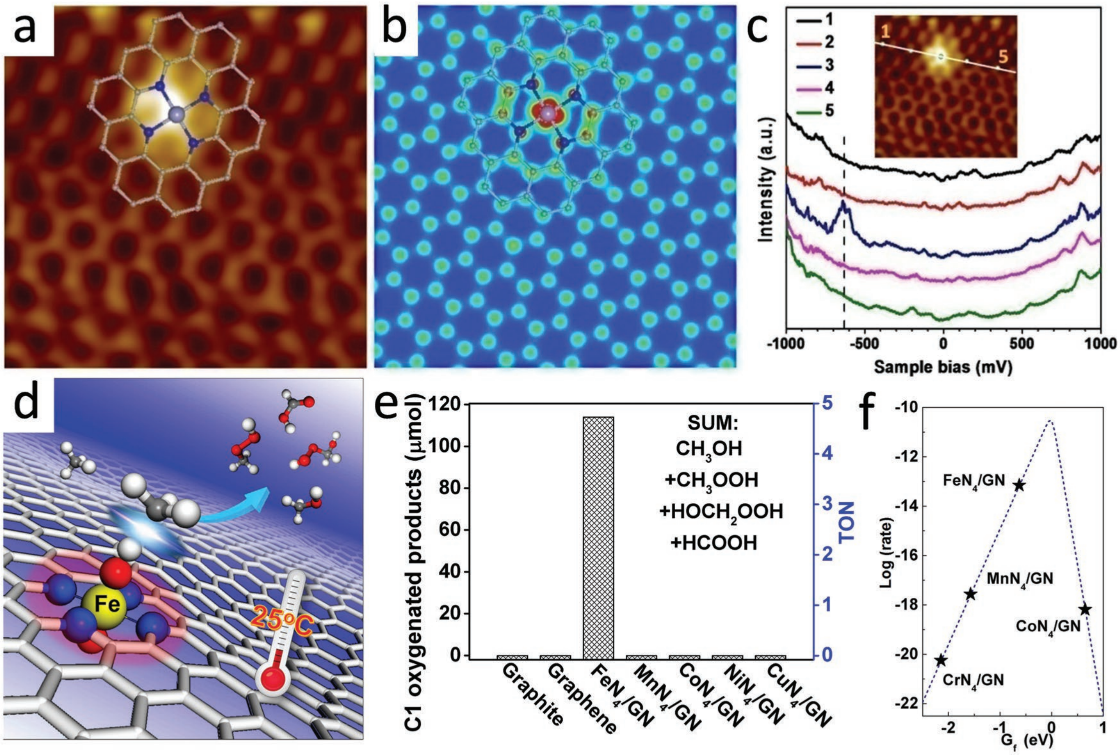

Figure 3. a) Scanning tunneling microscopy image of graphene confining FeN_4 site. b) Simulated scanning tunneling microscopy image for (a). c) Intensity profiles obtained from the mark line for (a). d) A sketch map of the catalytic process (shown here is CH_4 oxidation) on the surface of graphene confining FeN_4 center. e) Reaction activity of graphene confining FeN_4 center and other related catalysts for CH_4 oxidation. f) The relationship between the CH_4 activation rate and the formation free energy of the different catalytic site with a volcano curve. a–c) Reproduced with permission.[37] Copyright 2015, American Association for the Advancement of Science. d–f) Reproduced with permission.[52] Copyright 2018, Elsevier Inc.

ORR reaction.[21] In addition, the formation of B—C chemical bondings and N—C chemical bondings within the lattice of graphene is essential to understand the synergistic effect of N-doping and B-doping. Large-scale synthesis of B or N co-doping graphene has also been showed via a postannealing process. Qiao and co-workers revealed a new method to synthesize B,N-graphene without h-BN domains by employing a unique two-step sequential N or B doped process (Figure 2c).[22] The new nanocatalyst exhibited high catalytic activity in the ORR. The graphene confining B and N also exhibited higher catalytic performances than B/N-separated doping graphene in ORR (Figure 2d). Despite tremendous progress in the production of graphene confining nonmetal atoms,[23–26] a phase pure B/N co-doping graphene has not been fully realized, which makes the identification of the function of heteroatoms very difficult. Future work should focus on developing a graphene-based nanostructured catalyst at atom precision doping.

2.1.2. Graphene Confining Metal–N_x Centers

Since Jasinski reported that cobalt phthalocyanine could catalyze some electrocatalytic reactions in 1964, metal–N_x centers have been widely reported as effective nanocatalysts for a series of chemical catalytic processes.[27] It has been demonstrated that the coordinatively unsaturated metal centers are key to the high catalytic reaction. Graphene confining metal–N_x centers provides a promising strategy to not only take advantage of the catalytic activity of metal–N_x centers but also prevent their aggregation. So far, three types of the synthesis methods for graphene confining metal–N_x centers have been developed including pyrolysis, ball milling, and post treatment on pristine graphene. Pyrolysis of N,C-containing molecules and metal precursor is a common method to synthesize graphene confining metal–N_x catalysts.[28–36] In this process, templates such as SiO_2,[28–30] MgO,[33] and α-FeOOH,[31] have been widely used as supporting solids to synthesize graphene confining metal–N_x. However, these routes involve tedious synthetic processes, including the adsorption of metal precursors, followed by reduction and removal of templates. The reported synthesis routes were also relatively difficult to scale up because of the complex operating steps and sensitive conditions. Ball-milling approach is a simple and practical strategy to synthesize graphene confining metal–N_x, which was firstly reported by Deng et al. (**Figure** 3a–c).[37,38] Firstly, the graphene was cut by ball milling into small nanosheets. Then, these small nanosheets after mixing together an amount of metal phthalocyanine were treated with ball milling under inert gases atmosphere. Under the high energy input during the ball milling, metal–N_x centers could be introduced into the defects of graphene to obtain graphene confined metal–N_x. Up to now, a series of metals including Fe, Cu, Mn, and Co, have been successfully embedded into the lattice of graphene nanosheets through ball milling. Finally, post treatment is another facile method to synthesize graphene confining metal–N_x by heat treating of graphene and metal precursor in the presence of NH_3.[39–41]

Water splitting, as a promising strategy for hydrogen production, has received intense attention. Presently used catalysts for OER, a key reaction in water splitting technologies, typically require high-cost noble metal oxides. Graphene confining metal–N_x have been demonstrated as promising noble-metal-free catalyst for OER.[42,43] Guan et al. synthesized the single MnN_4 centers doped in the lattice of graphene (MnN_4-G), which showed a lower electrochemical overpotential in OER.[42] Density functional theory (DFT) results exhibited that the theoretical overpotential of MnN_4-G is much lower than that of a trinuclear Mn_3N_7-G. The difference in overpotential between MnN_4-G and Mn_3N_7-G was assigned to the over-destabilization of OOH* intermediate on Mn_3N_7-G. Other models of active sites also exhibited higher overpotential than MnN_4-G. These comparisons gave strong support to the vital responsibility and necessity of the mononuclear Mn site coupled to four N coordination environments for the superior catalytic activity of MnN_4-G.

The fuel cell is regarded as promising energy conversion devices, where the cathode reaction (ORR) is the major obstacle for improving the conversion efficiency of this energy-related device. Graphene confining metal–N_x have been also widely used for ORR. As reported by Deng and co-workers, the ORR catalytic performance of graphene confining FeN_4 centers were comparable to those of the typical Pt/C nanocatalyst.[44] In addition, the graphene confining FeN_4 exhibited a higher stability than Pt/C nanocatalysts. DFT results showed that the unique structure and high density of FeN_4 centers within the lattice of graphene can turn their catalytic activity. Yang et al. recently proposed an efficient and universal surfactant assisted method to synthesize the graphene confining metal–N_4 catalyst.[45] The onset potentials and half-wave potentials of ORR reach 1.0 V (vs reversible hydrogen electrode) and 0.88 V in alkaline condition while they are 0.9 and 0.8 V in acidic condition, respectively. Moreover, graphene confining metal–N_4 exhibited extremely high stability. Interestingly, the DFT results demonstrated that the doping of Fe-pyrrolic-N moieties was the major reason for high-ORR activity of graphene confining metal–N_4, which was unusual comparing to the common results. Although graphene confining FeN_4 structure was usually regarded as active site, the direct observation and confirmation of this active site structure was rarely achieved. Recently, Zelenay and co-workers. revealed that the carbon-embedded FeN_4 center was directly confirmed with aberration-corrected scanning transmission electron microscopy (AC-STEM), and the origin of catalytic centers within the lattice of graphene were elucidated through DFT calculations.[46] Besides the FeN_4 centers, the coordination environments of graphene can also be used to tune the catalytic performances of other metal–N_4 centers (CoN_x, CuN_x, MnN_x, and RuN_x) for ORR.

C1 molecules such as methane, carbon oxides, and oxygenated hydrocarbons are promising feedstock for the production of high value chemicals. CO_2, as the main greenhouse gas and the most abundant C1 molecules, has great effects on climate and environment.[47] CO_2 utilization research has gained a significant attention in recent decades. Previous research results have demonstrated that graphene confining metal–N_x could also be used as efficient catalysts for activating CO_2. Yang et al. reported that graphene confining NiN_x can be used as a promising catalyst for the conversion of CO_2.[48] The graphene confining NiN_4 exhibited high CO_2 reduction activity, reaching a high current at a low overpotential with 97% CO Faradaic efficiency. Furthermore, the graphene confining NiN_4 exhibited long-term stability. So far, graphene confining NiN_x have been widely reported for the CO_2 reduction.[49,50] Owing to its low price and high reserves, CH_4 distributed in shale gas or natural gas is widely used as one of the most important C1 resources.[51] However, CH_4 conversion to high-value products represents a great challenge in catalytic researching, which usually requires high-energy import to activation and conversion of CH_4 molecules due to the high reaction barrier. One of the pioneering works was reported by Deng and co-workers in 2018. In this work, graphene-confined FeN_4 centers can be used as promising catalyst to activate CH_4 molecules to high value products at low temperature (25 °C) (Figure 3d,e).[52] DFT calculations revealed that CH_4 is first converted methyl radicals by the O–FeN_4–O catalytic site and subsequently into value-added oxygenated products (Figure 3f).

2.1.3. Graphene Confining Metal Atoms

Previous reports showed that pure metal atom could also be anchored on graphene for tuning the catalytic performance of pristine graphene. For instance, Zhang et al. demonstrated that graphene confining single niobium atoms showed high ORR activity, since graphene confining the niobium heteroatoms led to the reconstitution of d-band electrons and became surprisingly active for oxygen activation.[53] Chen and co-workers demonstrated that graphene confining pure Ni single atoms can be prepared by acid-leaching method.[54] The authors revealed that Ni heteroatom occupied the position of one C atom and bonded with other C atoms within the basal planes of 2D graphene. Compared with graphene and conventional Ni-based catalysts, graphene confining pure Ni showed high HER performances together with long time stability in acidic condition. DFT results demonstrated that the superior catalytic performance of graphene confining Ni atom was created by synergetic effect between the Ni heteroatoms and the neighboring C atoms. Recently, Yao and co-workers also showed a similar method to synthesize graphene confining Ni atom catalysts.[55] Defects on graphene were used to trap atomic Ni species. Theoretical investigations based on the three typical doping models of Ni–C configuration revealed that the reaction mechanism of HER and OER have close relationship with Ni–C coordination conditions and is different from conventional Ni–N–C catalyst.

2.2. MoS_2 Confining Single Atoms

2D MoS_2 has gained great research interest in catalysis due to its well-defined structures and unique electronic properties.[56] Single-layer MoS_2 consists of three atomic layers, where Mo layer is sandwiched by two S layers. Coordinatively unsaturated edge atom of MoS_2 is known to provide active site for catalysis, whereas coordinatively saturated site on basal planes of 2D

MoS_2 is regarded as catalytically inert. We have proposed to turn the catalytic property of basal plane of 2D MoS_2 by doping heteroatoms to trigger the number of catalytically sites.[57,58] Here we will summarize two kinds of MoS_2 confining single atom nanocatalysts. One is single metal atom substituting Mo to trigger the catalytic activity of the adjacent S atoms, another is direct substitution of S atoms in the outer layer.

2.2.1. MoS_2 Confining Mo-Substituted Single Atoms

It is usually difficult to synthesize MoS_2 confining Mo-substituted single metal atoms by a post treatment way, owing to the six-coordinated Mo atoms are enclosed by two S layers. Thus, in situ method is a popular way for preparing MoS_2 confining Mo-substituted single metal atoms. Deng et al. firstly reported an in situ method to promote the HER catalytic activity of inert MoS_2 basal planes through single Pt atoms replacing Mo atoms in the lattice of few-layer MoS_2 (**Figure 4**a).[57] Theoretical investigations revealed that the Pt heteroatoms could modulate the adsorption free energy of H intermediates on the adjacent S atoms and therefore improve HER catalytic activity, which originates from the new electronic properties of MoS_2 confining Pt atoms. Moreover, the HER catalytic activity of MoS_2 doping with several single metal heteroatoms were explored by theoretical calculations, suggesting that the relationship between heteroatoms and the adsorption energy of H intermediates presented a volcano curve in HER (Figure 4b). Such electronic difference led to significantly different adsorption energy of H intermediates and consequently resulting in diverse HER catalytic activity, which was further confirmed in experiment by using Pt, Co and Ni heteroatoms doped MoS_2 as catalysts (Figure 4c). Furthermore, Deng et al. reported a multiscale strategy to synthesize MoS_2 confining Co atoms for HER.[58] Experimental results and DFT calculations demonstrated that an appropriate content of Co heteroatoms can considerable improve the HER performance of MoS_2. In addition, Xia and co-workers proposed a way to trigger the HER activity of MoS_2 by engineering its structural and electronic properties via heteroatom doping.[59] Zn-doped MoS_2 was synthesized as a typical example to understand the catalytic mechanism of HER. Theoretical calculations on the catalytic mechanism of this process revealed that the enhancement of catalytic performance was due to the synergistic effect of structural advantages (rich active sites) and novel electronic properties (transition-metal doping). Recently, Jia and co-workers also proposed a simple and practical method to activate the basal planes of MoS_2 for HER through introducing earth-abundant Zn elements into the lattice.[60] DFT calculations revealed that the doping Zn heteroatoms not only reduced the formation free energy of S-vacancy sites, but

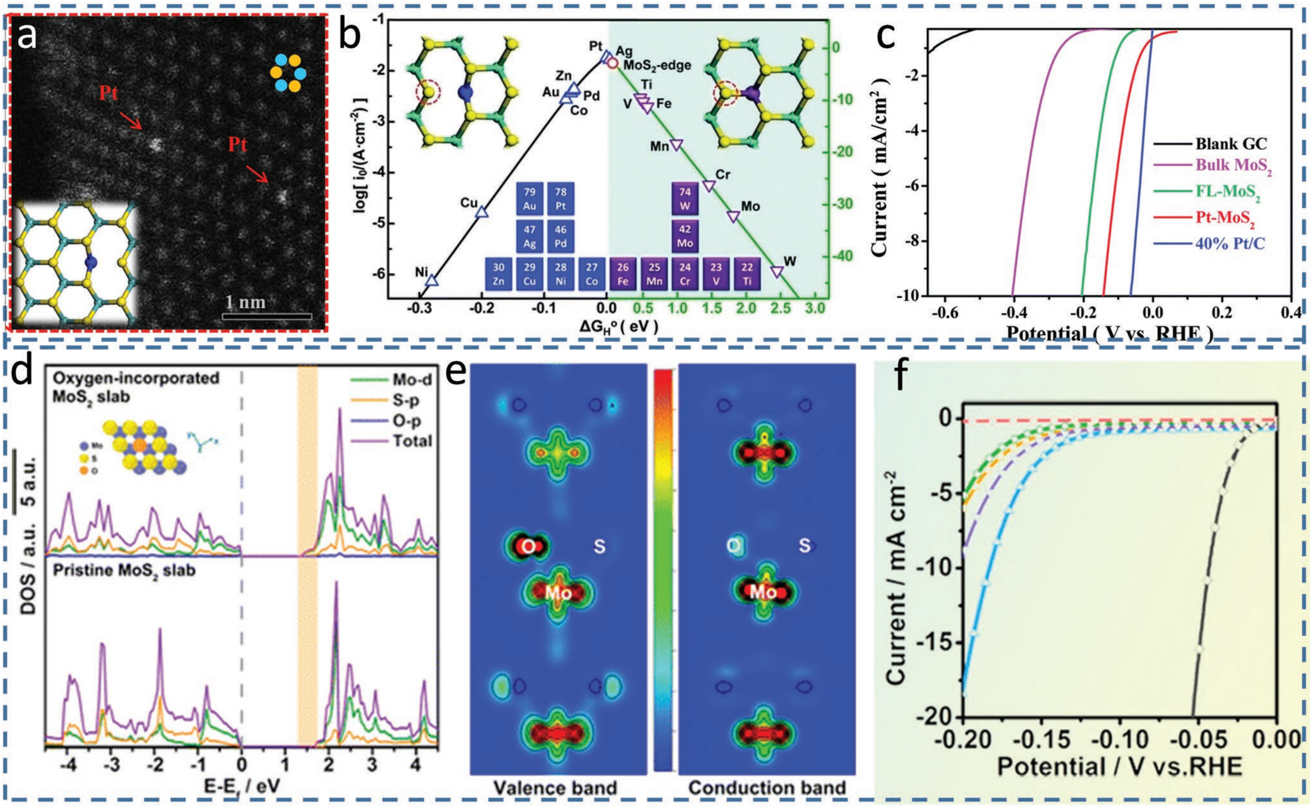

Figure 4. a) HR-STEM image of MoS_2 confining Pt single heteroatoms. The inset in (a) is the doping configuration of MoS_2 confining Pt single heteroatoms. b) The relationship between $\Delta G_H{}^{\circ}$ and currents ($\log(i_0)$) shows a volcanic curve when using MoS_2 with a series of single metal heteroatoms as catalyst. c) LSV curves of HER reaction for Pt-doped MoS_2 in comparison with referencing samples. d) The pure MoS_2 (bottom) and the calculated density of states of the O-doped MoS_2 (top). e) The density distributions of valence band (left) and conduction band (right) near the O atom in O-doped MoS_2, respectively. f) LSV results of the O-doped MoS_2. a–c) Reproduced with permission.[57] Copyright 2015, Royal Society of Chemistry. d–f) Reproduced with permission.[63] Copyright 2013, American Chemical Society.

also helped to lower the adsorption free energy of H atoms on the S-vacancy site. The optimal MoS_2 confining Zn showed an obviously enhanced HER performance compared to unreduced MoS_2 nanosheets. Moreover, rhenium (Re) can also be used as effective heteroatom to trigger neighboring S atoms for turning the adsorption energy of H intermediates, which was reported by a recent works.[61] The 50% Re-50% Mo (Re,Mo)S_2 nanoalloy showed the best HER performance compared with other samples. This new catalyst has enhanced HER catalytic activity with a small Tafel slope and a low overpotential.

2.2.2. MoS_2 Confining S-Substituted Single Atoms

The nonmetal atoms (O, N, P, Se, etc.) can be introduced into the lattice of MoS_2 by substituting S atoms. Unlike Mo-substituted single metal heteroatoms, the exposed nonmetal heteroatoms can not only directly activate the neighboring S atoms within the basal planes of MoS_2, but also act as new catalytic sites in HER. Xue and co-workers demonstrated that the doping P heteroatoms could be used as the new catalytic sites and help promote the intrinsic electronic conductivity, resulting in a greatly enhance the HER catalytic activity.[62] This work provided a novel way for turning the catalytic activity by P-doping. However, some results revealed that O atoms within the lattice of MoS_2 can only be used as heteroatoms to modulate the in-plane S atoms. For instance, Xie and co-workers discovered that MoS_2 confining O atoms with controllable disorder engineering realized the turning of active sites for efficient HER.[63] The optimized nanocatalyst showed extremely high activity and long-term durability. Theoretical calculations showed that the O heteroatoms can effectively affect the electronic states of neighboring S atoms and therefore promote the intrinsic catalytic properties of MoS_2 (Figure 4d,e). In addition, Ding and co-workers showed an economical and efficient way to synthesize N-doped MoS_2 nanosheets, which showed the dramatically enhanced activity in HER.[64] Moreover, DFT calculations revealed that the N heteroatoms activated the neighboring S sites for HER process and enhanced electronic conductivity of the basal plane.

2.3. g-C_3N_4 Confining Single Atoms

Graphitic carbon nitride, as typical 2D material with well-defined layered nanostructure, is useful owing to its visible-light response, physicochemical stability, and low cost with earth-abundant C and N elements.[65] Other nonmetal heteroatoms can be embedded into the basal planes of g-C_3N_4 via replacing C or N atoms which is same as the B,N atoms co-doping of graphene. Given that nonmetal atoms doping g-C_3N_4 has been reviewed by some recent reviews,[66] here the research progresses of single metal heteroatoms doping g-C_3N_4 will be only introduced. In photocatalysis, the catalytic performance of pristine g-C_3N_4 is usually limited by its drawbacks like the low energy conversion efficiency and the easy reconstruction of electron–hole pairs. Recent results have demonstrated that single metal heteroatoms doping g-C_3N_4 is a simple and practical way to boost the photocatalytic performances of g-C_3N_4. For instance, Wu and co-workers revealed that g-C_3N_4 confining Pt atoms can remarkably promote the photocatalytic performances, with a higher H_2 generation rates than those of pristine g-C_3N_4.[67] The synergetic interaction between Pt-atom co-catalyst and neighboring atoms within the lattice of g-C_3N_4 provided a useful way to modulate the catalytic properties of pristine g-C_3N_4. In addition, Xiong and co-workers also showed that the charge transfer between single Pt heteroatoms and g-C_3N_4 had great effect on the photocatalytic process.[68] g-C_3N_4 confining single Pt^{2+} also exhibited higher hydrogen generation rates than those of pristine g-C_3N_4. The DFT calculations showed that the excited electrons on Pt single atoms were transferred to the neighboring atoms of g-C_3N_4 which cause the formation of the novel electronic states. In addition, the introduction of nonprecious metal atoms into g-C_3N_4 can also be used to boost the catalytic performances of pristine g-C_3N_4. For example, Wei and co-workers showed that g-C_3N_4 confining single Co_1–P_4 site was prepared by a facile phosphorization method (**Figure 5**a–d), which exhibited high catalytic performances for overall water splitting (Figure 5e).[69b] The atomically dispersed Co_1–P_4 catalytic sites allowed efficient charge transfer from g-C_3N_4 to active sites, and finally lead to a high catalytic activity of overall water splitting. Likewise, g-C_3N_4 confining single Co_1–N_4 site have also been reported as a typical photocatalyst for high hydrogen production.[69a] DFT calculations showed that the nearby nitrogen donors turned the electronic states of active sites and lowered the energy barrier of catalytic key intermediate, thus boosting H–H coupling to promote the hydrogen production. In short, single metal heteroatoms doping g-C_3N_4 is a simple and practical way for synthesizing high-performance nanocatalysts by utilizing the synergetic effect between different single metal atoms and g-C_3N_4, which could catalyze a series of important catalytic reactions.

2.4. Other 2D Materials Confining Single Atoms

The strong interaction between 2D material and heteroatoms will unavoidably affect catalytic performances of energy conversion. Generally, different 2D material may lead to the properties of catalyst differently. The other 2D nanomaterials like graphdiyne, MXene, and ultrathin TiO_2 nanosheets, have also been used as support for confining single heteroatoms. As a novel allotrope of 2D carbon materials, graphdiyne has been adopted in various applications. Recently, Li and co-workers introduced a novel structure of N-doped configurations—sp-hybridized N (sp-N) heteroatoms into lattice of graphdiyne nanosheets, via pericyclic replacement of the acetylene chemical bonding.[70] The as-synthesized sp-N-doping graphdiyne exhibited high ORR activity, together with excellent cycling stability. Furthermore, DFT calculations demonstrated that these catalytic performances originated from sp-N heteroatoms, which could effectively affect the electronic states of neighboring single atoms and thus enhance the intrinsic catalytic properties of the catalyst. Interesting, $Mo_2TiC_2T_x$ MXene nanosheets with abundant surface Mo vacancies by electrochemical exfoliation have recently been reported as support to trap Pt heteroatoms (**Figure 6**a,b).[71] The resultant $Mo_2TiC_2T_x$–Pt catalysts showed a high catalytic activity with a low overpotentials and a mass activity about 40 times higher than that of Pt/C nanocatalyst (Figure 6c).

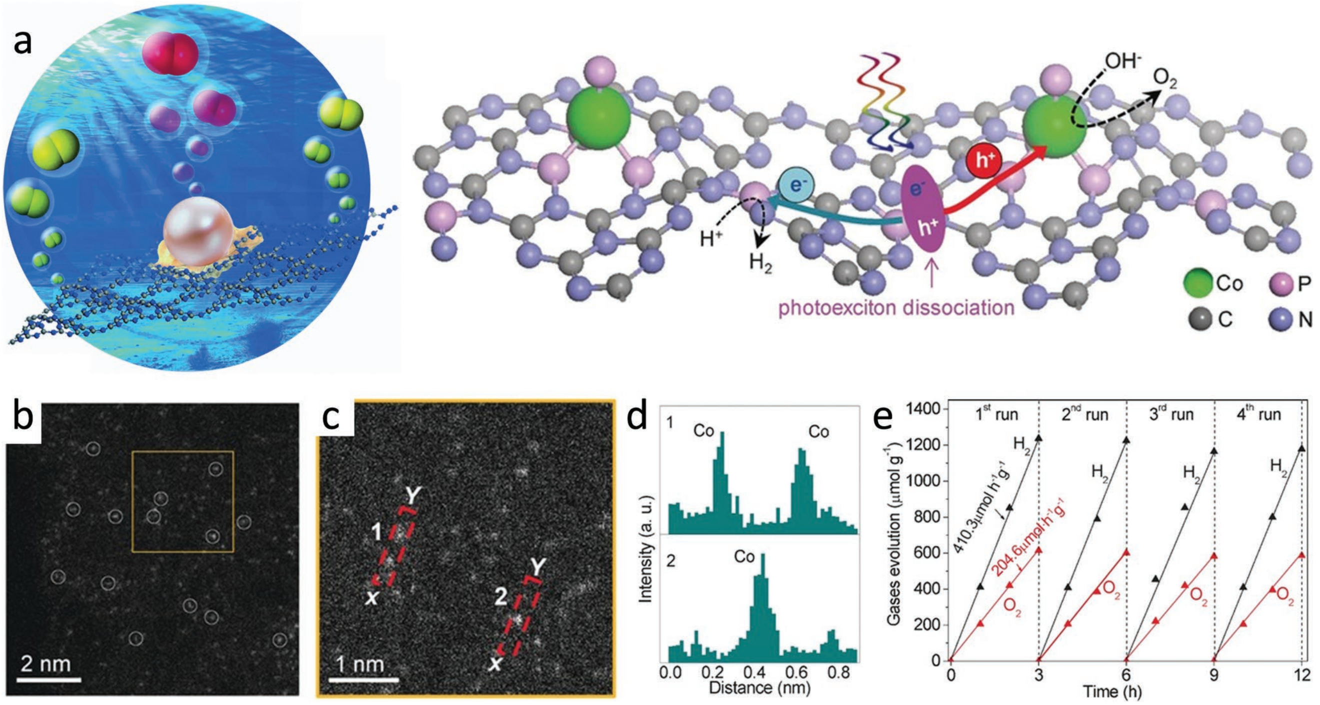

Figure 5. a) Sketch map of the sunlight-driven overall water splitting on g-C_3N_4 confining Co1–phosphide catalyst, in which the photogenerated electrons and holes are spatially separated, and charge transferred to Co1–phosphide to drive HER and OER. b) STEM image of g-C_3N_4 confining Co1–phosphide catalyst. c) STEM image acquired from the area in (b). d) Intensity profiles acquired from the red lines 1 and 2 in (c). e) Catalytic performances of water splitting by g-C_3N_4 confining Co1–phosphide catalyst. Reproduced with permission.[69b] Copyright 2017, Wiley-VCH.

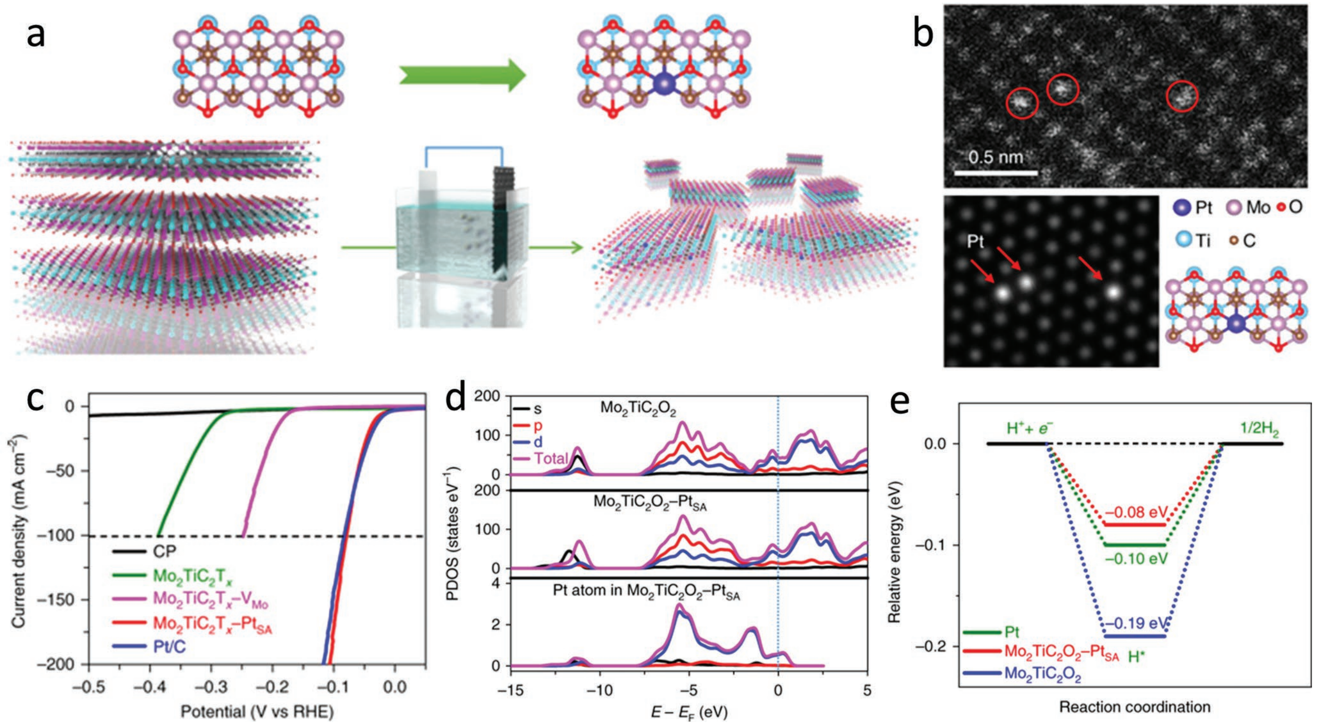

Figure 6. a) The electrochemical exfoliation process of MXene with confined single Pt heteroatoms. b) HRTEM image of Pt-doped MXene and its related simulated image. c) HER curves of Pt-doped MXene and other related nanocatalysts. d) Calculated PDOS of MXene and Pt-doped MXene. e) Free energy profiles of HER at the equilibrium potential of MXene, Pt-doped MXene and Pt/C. Reproduced with permission.[71] Copyright 2018, Springer Nature.

Theoretical calculations suggested that Pt heteroatoms with positively charged anchored on MXene comprised the optimum adsorption position for H^+, which facilitates H_2 production (Figure 6d,e). The ultrathin TiO_2 nanosheets represent a promising supports to trap heteroatoms owing to the simple and well-defined structure.[72] Wang and co-workers showed a simple and practical way to support single Au atoms by creating defects on the basal planes of TiO_2 nanosheets.[73] The resulted Ti–Au–Ti chemical nanostructure could improve the catalytic performances via lowering the formation barrier and restraining the competitive reaction on single Au atoms. In summary, 2D materials confining single atoms opens an alternative avenue for developing highly efficient single-atom catalysts.

3. Catalysis with 2D Cover-Confined Metals

The confinement effect not only includes the modulation of electronic state by the confinement environment at atomic-scale, it also refers to the control of electronic states or reaction space at nanoscale. The gap of work functions between 2D cover and confined metal leads to the charge penetration from metal to 2D cover to trigger the catalytic activity at outer surface. Moreover, the interface of 2D cover and metal can also provide a confined space to allow the control of diffusion and interaction of catalytic reactants on the surface of inner nanometal catalysts. In this section, catalytic reactions over 2D cover with metals encapsulation and in the confined space between 2D cover and metals will be introduced.

3.1. Catalytic Reactions over 2D Cover on Metals

Considering that noble metals exhibit inimitable performance over other catalysts in catalysis, they are usually employed to drive a series of energy-related chemical reactions.[74] The high cost and low efficiency of precious metal-based nanocatalysts, however, are major barriers for large-scale industrial applications. Considerable efforts have been made for the development of non-noble-metal-based nanocatalysts. Although non-noble metal catalysts may have the surpassing or comparable catalytic performances in a number of catalytic processes,[75] one major problem in non-noble metal nanocatalysts is their poor stability in harsh reaction conditions (e.g., high overpotential, high temperature, and strong acidity or alkalinity). Therefore, it is a great challenge to keep high stability of the non-noble metal nanocatalysts without impairing catalytic performances under harsh reaction processes. Constructing 2D cover encapsulating non-noble metal catalysts (chainmail catalysts) has been proposed as a promising strategy by our group (**Figure 7**a).[76] In the chainmail catalyst, the graphene cover boosts the electron penetration from encapsulated nanometals to the inert graphene, while the outer cover can also completely protect the encapsulated nanometals from damage under harsh reaction processes. This unique strategy can promote both the catalytic activity and stability of inner nanocatalysts,[76] which has been vividly described as“chainmail for catalyst.”Encouragingly, previous research has confirmed that electron transfer from inner metals affected the catalytic reactions of the inert graphene. Like graphene, other 2D materials (hBN, $g\text{-}C_3N_4$, etc.) can be also adopted to encapsulate the non-noble-metal-based materials. Benefiting from the advantages of 2D cover encapsulating metal, the chainmail catalysts have been extended into many important catalytic processes under harsh conditions.

3.1.1. The Chainmail Catalysts for ORR

Graphene encapsulating metal has the overwhelming advantage to replace Pt-based noble electrocatalysts in ORR reaction because of the low cost and the high stability under working conditions. For example, Deng and co-workers reported that graphene cover encapsulating Fe nanoparticles exhibited both high activity and high stability (Figure 7b,c).[76a] Experiments and DFT calculations revealed that electron could transfer from the metallic Fe nanoparticles to the inert cover due to the work function difference between outer cover and the inner nanometal. The electron penetration led to the change of local electronic state on outer shell, which promoted oxygen activation on graphene shell. Thus, the graphene cover can be used to protect non-noble metal catalysts in harsh reaction conditions, while the catalytic performance of inner nanometal will not be shielded by outer cover. Since then, more non-noble metals were successfully covered by graphene shell for the ORR. Li and co-workers systematically showed a general way to synthesize graphene confining transition metal nanoparticles.[77] The different transition metals exhibited different promotion to the ORR performances, where N-doped graphene encapsulated Co nanoparticles even showed a higher catalytic activity than noble-metal-based catalyst along with good stability under harsh reaction conditions. In addition to metallic non-noble metal, many kinds of non-noble-metal-based nanomaterials have also been successfully enclosed into the graphene shell for various energy-related catalytic reactions, like metal carbide, metal oxide, metal phosphide, etc. For instance, Hu et al. reported a new ORR nanocatalyst with a well-controlled hollow sphere structure comprising uniform Fe_3C nanoparticles covered by graphene shell.[78] These unique catalysts showed excellent activities and high stabilities toward ORR. The graphene shell stabilized the inner Fe_3C nanoparticles in hot acids and the electron penetration from inner Fe_3C nanoparticles activated the outer surface toward ORR.

3.1.2. The Chainmail Catalysts for HER

Electrochemical water splitting requires inexpensive electrocatalysts with low HER overpotential. Although Pt-based catalysts have excellent catalytic performances, the high cost hampers their large-scale utilization. The chainmail catalysts show potentials to substitute Pt or Pt-based catalysts and were firstly studied by our group and Laasonen's group recently. Deng et al. reported a way to introduce transition metals into carbon nanotubes for HER.[79] The optimized catalysts exhibited superior activity and long-term durability, which is even comparable to those of the typical Pt/C nanocatalyst. DFT results demonstrated that encapsulation of nanometal and the introduction N-dopants could synergistically optimize both the

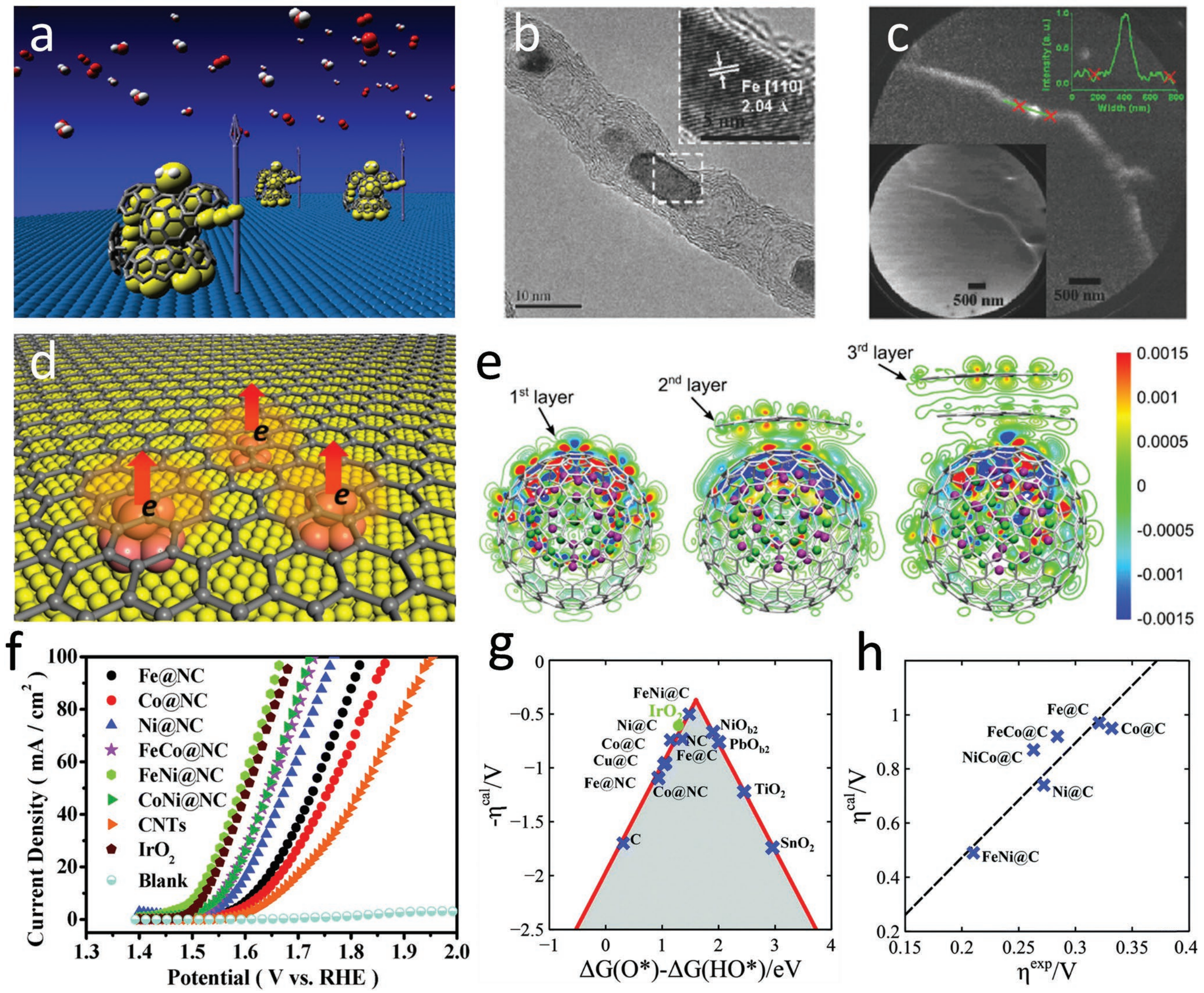

Figure 7. a) The concept of "chainmail for catalyst." b) HRTEM results of graphene confining Fe nanoparticle, inset shows the crystal plane of the encapsulated Fe nanoparticle. c) The picture of graphene confining Fe nanoparticle revealed by photoemission electron microscopy. The bottom inset of graphene confining Fe nanoparticle revealed by low-energy electron microscopy. The top image indicates the lightness profile along the green line. d) The schematic illustration of electron penetration through the outer graphene cover. e) The change of thickness from one to three graphene layers leads to the redistribution of electron density for graphene confining metals. f) LSV results for graphene encapsulating nanometal in comparison with other samples. g) The calculated negative overpotential for the universal descriptor ΔG(O*) – ΔG(HO*) on a series of graphene encapsulating metals. h) Calculated overpotential versus the experimental overpotential of different graphene encapsulating metals. a) Reproduced with permission.[5d] Copyright 2017, Wiley-VCH. b,c) Reproduced with permission.[76a] Copyright 2013, Wiley-VCH. d) Reproduced with permission.[5a] Copyright 2016, Springer Nature. e) Reproduced with permission.[80] Copyright 2015, Wiley-VCH. f–h) Reproduced with permission.[83] Copyright 2016, Royal Society of Chemistry.

electronic states of graphene shell and the adsorption energy of reaction intermediates on graphene shell, and thus improve the HER activity. However, the multilayer graphene shells are too thick to promote electron transfer which may significantly reduce the activity. To further promote the catalytic activity, Deng et al. showed a practical way to synthesize CoNi nanoalloy catalysts covered by outer graphene shell with only one to three graphene layers.[80] The unique catalyst exhibited high stability and activity in HER. DFT calculations indicated that graphene cover with only 1–3 layers strongly promoted electron penetration from the inner metal alloy to the outer cover (Figure 7d,e). Almost at the same time, Laasonen and co-workers also showed a unique way to synthesize single shell graphene-encapsulated Fe nanoparticles, which showed high catalytic performances for HER.[81] The catalytic performances of this chainmail catalyst demonstrated an acid-stable HER nanocatalyst with a high catalytic performance comparable to those of platinum. Besides the non-noble metals, other kinds of non-noble-metal-based materials like metal phosphide can also be encapsulated as HER catalyst. Recently, Sung and co-workers reported an effective method to synthesize graphene-shell-protected iron phosphide nanoparticles that have high catalytic performances for HER.[82] Experimental measurements and DFT results revealed that oxidation resistance of graphene cover on nanoparticles was the origin of the long-term durability.

3.1.3. The Chainmail Catalysts for OER

Graphene encapsulating metal also exhibited excellent performance for the OER under strong alkaline electrolytes. Deng and co-workers showed a simple and practical way for the production of single shell graphene confining uniform transition metals.[83] Experimental results revealed that different inner nanometals played a different role in the reaction process, and the optimized nanocatalyst showed high OER activity with a lower overpotential, which are even comparable to IrO_2 catalysts (Figure 7f). DFT results indicated that the electron penetration from the inner nanometals to the inert graphene regulated the electronic states of outer cover for OER activity (Figure 7g,h). Furthermore, Wang and co-workers also showed an effective electrospinning technology to synthesize small cobalt nanoparticle covered by graphene shell.[84] The excellent catalytic activity could be ascribed to the synergistic effect of N-doping and cobalt encapsulation. Likewise, Lou and co-workers showed a way to synthesize a hollow structure constructed from interconnected graphene-encasing inner metal starting with metal–organic frameworks particles as single precursor.[85] The resulted catalyst showed a lower overpotential, which compared to the typical IrO_2/C catalyst. The excellent catalytic activity might be attributed to the synergistic effect of the graphene-encasing inner metals and the unique hollow framework. These results revealed that the electronic states of outer shell could greatly modulate the OER reactivity, which highly rely on the types of inner nanometals and their related proportion. Generally, it is difficult to change the inner metals and their proportion within the graphene shell. Recently, Tu et al. showed an effective method to synthesize ultrathin graphene confining FeNi nanoalloy, which efficiently optimize the OER activity by changing Fe/Ni ratio.[86] The optimized nanocatalyst exhibited a low overpotential in OER. More importantly, the catalytic performances of the optimized nanocatalyst were better than those of IrO_2 catalysts. Theoretical calculations demonstrated that the electronic structure of the key intermediate on outer shell could be efficiently optimized by turning the proportion of the inner metal, resulting in an enhanced catalytic performance. In short, graphene encapsulating metal provided a promising strategy to synthesize active non-noble metal nanocatalysts for energy-related reaction processes. Chainmail catalysts exhibit high stability in the OER under alkaline electrolytes, but may suffer corrosion of the graphene shell under strong acid electrolytes. In this regard, increasing the carbon layer thickness could be a promising way to improve the stability of the catalyst in the OER under strong acid electrolytes.

3.2. Catalytic Reactions in the Confined Space between 2D Cover and Metal Surface

In the above section, we showed that the strong interaction between 2D cover and the inner metals helps to activate 2D cover, on which reactions can occur. On the other hand, catalytic reactions could occur in the confined space between 2D cover and inner nanometal surface when metals interact weakly with 2D cover (**Figure 8**a,b). Graphene and h-BN have been deposited on metal surfaces via surface transfer strategies. The weak interaction between 2D cover and metal via the van der Waals force leads to a moderate distance of within 1 nm between them, and thus small molecules can populate the confined space between 2D cover and metal surface.[87]

The confined nanospace between 2D cover and inner metal offers an ideal micro-environment for exploring the confinement catalysis experimentally and theoretically. For instance, Gao et al. presented a simple and practical synthesis way to encapsulate Ni nanoparticles within few-layer h-BN cover.[88] This unique catalyst exhibited an improved catalytic performance in the hydrogen oxidation reaction process compared with bulk metal nanoparticles (Figure 8c). The h-BN cover could modulate the interaction of the reaction intermediates on the inner metal surfaces. In situ evidence and DFT results demonstrated that the improved catalytic activity was ascribed to the confinement effect from the outer h-BN cover. Thus, the h-BN cover not only protected the inner Ni nanoparticles but also produced a confinement effect for the catalytic process. Taking advantages of DFT calculations, Zhou et al. investigated the catalytic performance of graphene-covered different nanometals in HER.[89] This result demonstrated that the interaction between the H atoms and active metals was modulated when H atoms were confined within the interface between outer cover and nanometal surfaces. In addition, using the surface of Pt(111)/graphene as the model, Fu and co-workers revealed that the interaction between atoms or small molecules and a Pt(111) surface always has been weakened under graphene-confined environments,[90] which was attributed to the confinement effect under graphene cover (Figure 8d). The confined environment between 2D cover and metal surface could be used to regulate catalytic reaction, which was further confirmed by optimizing ORR activity on Pt(111) covered by a series of 2D nanomaterials (Figure 8e). These findings demonstrate that confinement catalysis under 2D cover is an appealing catalytic platform for energy-related reactions.

4. Conclusion and Outlook

2D materials offer valuable host to construct high-performance catalysts for energy conversion. Here, we have introduced two major strategies, i.e., 2D lattice-confined single atoms and 2D cover-confined metal, which have been applied to construct 2D confinement catalytic systems. The regulation of the lattice of 2D materials and the interface between 2D cover and substrate have led to the desired confinement environment for active sites, thereby opening the door for applying confinement catalysis in energy-related catalytic processes, like water electrolysis, fuel cells, and C1 molecules transformation (**Table 1**). A combination of experimental studies and theoretical calculations are beneficial to the understanding of reaction kinetics of small energy-related molecules on 2D materials confined active sites.

2D lattice-confined single atoms have great significance in both experimental and theoretical researches of heterogeneous

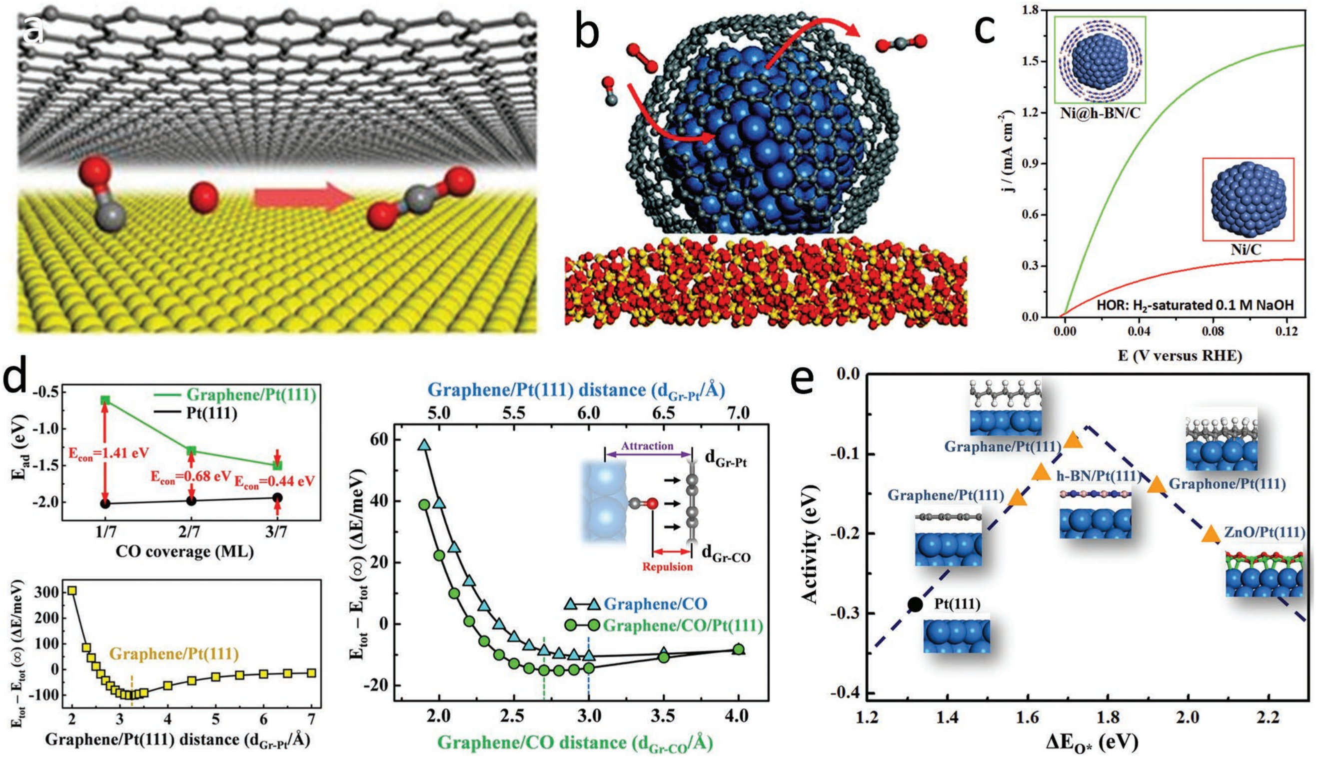

Figure 8. a) Schematic illustration of catalysis in the space between inner metal and 2D cover. b) catalysts encapsulated with 2D cover. c) LSV curves from the Ni@h-BN/C and Ni/C catalysts. d) The interaction between CO and Pt(111) surface under the confinement environments and the related confinement energy. e) A volcanic curve about the relationship between catalytic activity and absorption free energies of oxygen atoms (ΔE_{O*}) on Pt surface in ORR. a) Reproduced with permission.[5a] Copyright 2016, Springer Nature. b) Reproduced with permission.[91] Copyright 2017, Royal Society of Chemistry. c) Reproduced with permission.[88] Copyright 2017, Royal Society of Chemistry. d,e) Reproduced with permission.[90] Copyright 2017, The Authors, published by National Academy of Sciences.

Table 1. Summary of confinement catalysis with 2D materials for energy conversion.

Types of catalysts		Reaction system	Activity origin or mechanism	Performance
2D lattice-confined single atoms	Graphene confining nonmetal atoms	ORR in alkaline conditions[10b,11]	Nonmetal atoms can tune the charge distribution and electronic states of the adjacent C atoms, both hetero and C atoms can become the active sites	Catalytic activity is comparable to Pt/C
	Graphene confining metal–N_x centers	OER in alkaline conditions[42,43] ORR in alkaline conditions[44,45] C1 molecules (CO_2, CH_4) activation[48–52]	The unique electronic structure and high density of metal–N_x centers within the lattice of graphene	Catalytic activity is comparable to IrO_2 Catalytic performance is comparable to Pt/C Improved conversion of C1 molecules to high-value-added products and improved catalyst stability
	Graphene confining pure metal atoms	Electrocatalytic HER in acid[54]	Charge redistribution between the metal dopants and the surrounding C atoms	Higher activity and catalyst stability
	MoS_2 confining Mo-substituted single metal atoms	Electrocatalytic HER in acid[57,59–61]	Mo-substituted single metal atoms can trigger the adjacent S atoms of MoS_2	Performance increases with increasing dopants
	MoS_2 confining S-substituted single atoms	Electrocatalytic HER in acid[62,63]	Heteroatoms not only directly act as active centers but also activate the adjacent S atoms in MoS_2	Performance increases with increasing dopants
	g-C_3N_4 confining single atoms	Photocatalytic HER[67]	Charge redistribution between single heteroatoms and g-C_3N_4	50-fold enhancement in H_2 generation rate
2D cover-confined metals	2D materials encapsulating metal	ORR in acidic fuel cells[76a] HER in acid conditions[79–81] OER in alkaline conditions[83–86]	Electrons from inner metal sites can transfer to 2D cover, which could activate the surface electronic states and enhances activity	High catalyst stability. Enhanced catalytic activity
	Nanoreactor between metal surface and 2D cover	Hydrogen oxidation reaction in alkaline conditions[89]	The confinement effect from the outer 2D cover	Improved activity and stability

catalysis at the atomic scale. The following aspects should be paid more attention in the future study of 2D lattice-confined single atoms. 1) Novel methods and approaches should be developed to obtain catalysts with controllable compositions and coordination structure of single atoms. More convenient, economical, and scalable methods are highly required. 2) Decreasing the layer number of 2D materials could improve the utilization of active sites. The single-layer 2D nanomaterials confined single atoms have not been fully achieved. Thus, future research should focus on the precise synthesis of 2D lattice-confined single atoms with narrower distribution of layer numbers. 3) There are no well-established methodologies with which to reveal the structural information for 2D lattice-confined single atoms. Therefore, more efficient characterization methods should be developed to directly confirm the active sites at atomic level.

2D cover-confined metal centers provides a strategy to use non-noble metal catalysts in the catalytic processes under harsh conditions. Although considerable progress has been made in this research field, some challenges are yet to be overcome. First, there is still lack of an effective method to achieve the precise regulation and control of electronic and structural properties in the 2D materials confining metals. For example, method for accurately controlling the layer number of graphene or heteroatom doped graphene needs to be further explored. Second, many preparation processes are not economical due to the use of expensive precursors, high-temperature treatment, etc. Despite continuous efforts, the rapid and rational synthesis of 2D cover-confined metal catalysts with facile synthetic methods remains a challenge. Third, beyond graphene, other 2D materials confined metal catalysts should be explored. These 2D substrates can provide unique electronic states and different confinement environments for metals to design novel catalysts for diversified reactions.

Acknowledgements

The authors gratefully acknowledge the financial support from the Ministry of Science and Technology of China (nos. 2016YFA0204100 and 2016YFA0200200), the National Natural Science Foundation of China (nos. 21890753 and 21573220), the Key Research Program of Frontier Sciences of the Chinese Academy of Sciences (no. QYZDB-SSW-JSC020), and the DNL Cooperation Fund, CAS (no. DNL180201). This work is dedicated to the 70th anniversary of Dalian Institute of Chemical Physics, CAS.

Conflict of Interest

The authors declare no conflict of interest.

Keywords

2D materials, confinement catalysis, energy conversion, single atoms

Received: March 29, 2019
Revised: June 9, 2019
Published online:

[1] a) F. Bonaccorso, L. Colombo, G. Yu, M. Stoller, V. Tozzini, A. C. Ferrari, R. S. Ruoff, V. Pellegrini, *Science* **2015**, *347*, 1246501; b) S. Chu, A. Majumdar, *Nature* **2012**, *488*, 294; c) N. S. Lewis, D. G. Nocera, *Proc. Natl. Acad. Sci. USA* **2006**, *103*, 15729; d) J. A. Turner, *Science* **2004**, *305*, 972; e) K. K. Sakimoto, N. Kornienko, P. Yang, *Acc. Chem. Res.* **2017**, *50*, 476; f) X. H. Cao, C. L. Tan, M. Sindoro, H. Zhang, *Chem. Soc. Rev.* **2017**, *46*, 2660.

[2] a) Y. Jiao, Y. Zheng, M. Jaroniec, S. Z. Qiao, *Chem. Soc. Rev.* **2015**, *44*, 2060; b) Z. Huang, J. Song, L. Pan, X. Zhang, L. Wang, J. Zou, *Adv. Mater.* **2015**, *27*, 5309; c) B. You, M. T. Tang, C. Tsai, F. Abild-Pedersen, X. Zheng, H. Li, *Adv. Mater.* **2019**, *31*, e1807001.

[3] a) X. Pan, X. Bao, *Acc. Chem. Res.* **2011**, *44*, 553; b) Q. Fu, W. Li, Y. X. Yao, H. Liu, H. Su, D. Ma, X. Gu, L. Chen, Z. Wang, H. Zhang, B. Wang, X. Bao, *Science* **2010**, *328*, 1141; c) Q. Fu, F. Yang, X. Bao, *Acc. Chem. Res.* **2013**, *46*, 1692; d) J. Xiao, X. Pan, S. Guo, P. Ren, X. Bao, *J. Am. Chem. Soc.* **2015**, *137*, 477; e) F. Yang, D. Deng, X. Pan, Q. Fu, X. Bao, *Natl. Sci. Rev.* **2015**, *2*, 183.

[4] a) A. K. Geim, K. S. Novoselov, *Nat. Mater.* **2007**, *6*, 183; b) M. Xu, T. Liang, M. Shi, H. Chen, *Chem. Rev.* **2013**, *113*, 3766; c) C. Tan, X. Cao, X. Wu, Q. He, J. Yang, X. Zhang, J. Chen, W. Zhao, S. Han, G.-H. Nam, M. Sindoro, H. Zhang, *Chem. Rev.* **2017**, *117*, 6225; d) Y. Liu, Y. Huang, X. Duan, *Nature* **2019**, *567*, 323; e) N. Mounet, M. Gibertini, P. Schwaller, D. Campi, A. Merkys, A. Marrazzo, T. Sohier, I. E. Castelli, A. Cepellotti, G. Pizzi, N. Marzari, *Nat. Nanotechnol.* **2018**, *13*, 246; f) A. P. Balan, S. Radhakrishnan, C. F. Woellner, S. K. Sinha, L. Deng, C. de los Reyes, B. Manmadha Rao, M. Paulose, R. Neupane, A. Apte, V. Kochat, R. Vajtai, A. R. Harutyunyan, C.-W. Chu, G. Costin, D. S. Galvao, A. A. Martí, P. A. van Aken, O. K. Varghese, C. Sekhar Tiwary, A. M. M. R. Iyer, P. M. Ajayan, *Nat. Nanotechnol.* **2018**, *13*, 602.

[5] a) D. Deng, K. S. Novoselov, Q. Fu, N. Zheng, Z. Tian, X. Bao, *Nat. Nanotechnol.* **2016**, *11*, 218; b) Y. Sun, S. Gao, F. Lei, Y. Xie, *Chem. Soc. Rev.* **2015**, *44*, 623; c) H. Jin, C. Guo, X. Liu, J. Liu, A. Vasileff, Y. Jiao, Y. Zheng, S. Qiao, *Chem. Rev.* **2018**, *118*, 6337; d) J. Deng, D. Deng, X. Bao, *Adv. Mater.* **2017**, *29*, 1606967; e) Y. Wang, J. Mao, X. Meng, L. Yu, D. Deng, X. Bao, *Chem. Rev.* **2019**, *119*, 1806.

[6] a) Q. Fu, H. Saltsburg, M. Flytzani-Stephanopoulos, *Science* **2003**, *301*, 935; b) J. M. Thomas, R. Raja, D. W. Lewis, *Angew. Chem., Int. Ed.* **2005**, *44*, 6456; c) J. H. Kwak, J. Hu, D. Mei, C. Yi, D. H. Kim, C. H. F. Peden, L. F. Allard, J. Szanyi, *Science* **2009**, *325*, 1670; d) Y. Zhai, D. Pierre, R. Si, W. Deng, P. Ferrin, A. U. Nilekar, G. Peng, J. A. Herron, D. C. Bell, H. Saltsburg, M. Mavrikakis, M. Flytzani-Stephanopoulos, *Science* **2010**, *329*, 1633; e) B. Qiao, A. Wang, X. Yang, L. F. Allard, Z. Jiang, Y. Cui, J. Liu, J. Li, T. Zhang, *Nat. Chem.* **2011**, *3*, 634; f) X. Yang, A. Wang, B. Qiao, J. Li, J. Liu, T. Zhang, *Acc. Chem. Res.* **2013**, *46*, 1740; g) C. Zhu, S. Fu, Q. Shi, D. Du, Y. Lin, *Angew. Chem., Int. Ed.* **2017**, *56*, 13944; h) S. Wei, A. Li, J. Liu, Z. Li, W. Chen, Y. Gong, Q. Zhang, W. Cheong, Y. Wang, L. Zheng, H. Xiao, C. Chen, D. Wang, Q. Peng, L. Gu, X. Han, J. Li, Y. Li, *Nat. Nanotechnol.* **2018**, *13*, 856; i) Y. Gao, Z. Cai, X. Wu, Z. Lv, P. Wu, C. Cai, *ACS Catal.* **2018**, *8*, 10364.

[7] K. Gong, F. Du, Z. Xia, M. Durstock, L. Dai, *Science* **2009**, *323*, 760.

[8] a) X. Wang, G. Sun, P. Routh, D. H. Kim, W. Huang, P. Chen, *Chem. Soc. Rev.* **2014**, *43*, 7067; b) X. Kong, C. Chen, Q. Chen, *Chem. Soc. Rev.* **2014**, *43*, 2841; c) Y. Jiao, Y. Zheng, K. Davey, S. Qiao, *Nat. Energy* **2016**, *1*, 16130.

[9] L. Song, Z. Liu, A. L. M. Reddy, N. T. Narayanan, J. Taha-Tijerina, J. Peng, G. Gao, J. Lou, R. Vajtai, P. M. Ajayan, *Adv. Mater.* **2012**, *24*, 4878.

[10] a) L. Yu, X. Pan, X. Cao, P Hu, X. Bao, *J. Catal.* **2011**, *282*, 183; b) L. T. Qu, Y. Liu, J.-B. Baek, L. M. Dai, *ACS Nano* **2010**, *4*, 1321.

[11] D. Deng, X. Pan, L. Yu, Y. Cui, Y. Jiang, J. Qi, W. Li, Q. Fu, X. Ma, Q. Xue, G. Sun, X. Bao, *Chem. Mater.* **2011**, *23*, 1188.

[12] a) C. Zhang, R. Hao, H. Liao, Y. Hou, *Nano Energy* **2013**, *2*, 88; b) L. Dai, Y. Xue, L. Qu, H. J. Choi, J. B. Baek, *Chem. Rev.* **2015**, *115*,

4823; c) J. M. Gottfried, K. Flechtner, A. Kretschmann, T. Lukasczyk, H.-P. Steinrück, *J. Am. Chem. Soc.* **2006**, *128*, 5644.
[13] J. Wu, M. F. Rodrigues, R. Vajtai, P. M. Ajayan, *Adv. Mater.* **2016**, *28*, 6239.
[14] E. J. Biddinger, U. S. Ozkan, *J. Phys. Chem. C* **2010**, *114*, 15306.
[15] S. Ratso, I. Kruusenberg, M. Vikkisk, U. Joost, E. Shulga, I. Kink, T. Kallio, K. Tammeveski, *Carbon* **2014**, *73*, 361.
[16] D. Guo, R. Shibuya, C. Akiba, S. Saji, T. Kondo, J. Nakamura, *Science* **2016**, *351*, 361.
[17] L. Yang, S. Jiang, Y. Zhao, L. Zhu, S. Chen, X. Wang, Q. Wu, J. Ma, Y. Ma, Z. Hu, *Angew. Chem., Int. Ed.* **2011**, *50*, 7132.
[18] J. Jin, F. Pan, L. Jiang, X. Fu, A. Liang, Z. Wei, J. Zhang, G. Sun, *ACS Nano* **2014**, *8*, 3313.
[19] L. Ci, L. Song, C. Jin, D. Jariwala, D. Wu, Y. Li, A. Srivastava, Z. F. Wang, K. Storr, L. Balicas, F. Liu, P. M. Ajayan, *Nat. Mater.* **2010**, *9*, 430.
[20] S. Wang, L. Zhang, Z. Xia, A. Roy, D. W. Chang, J.-B. Baek, L. Dai, *Angew. Chem., Int. Ed.* **2012**, *51*, 4209.
[21] Y. Gong, H. Fei, X. Zou, W. Zhou, S. Yang, G. Ye, Z. Liu, Z. Peng, J. Lou, R. Vajtai, B. I. Yakobson, J. M. Tour, P. M. Ajayan, *Chem. Mater.* **2015**, *27*, 1181.
[22] Y. Zheng, Y. Jiao, L. Ge, M. Jaroniec, S. Z. Qiao, *Angew. Chem., Int. Ed.* **2013**, *52*, 3110.
[23] a) S. Agnoli, M. Favaro, *J. Mater. Chem. A* **2016**, *4*, 5002; b) H. Wang, T. Maiyalagan, X. Wang, *ACS Catal.* **2012**, *2*, 781.
[24] J. Shui, M. Wang, F. Du, L. Dai, *Sci. Adv.* **2015**, *1*, e1400129.
[25] C. H. Choi, M. W. Chung, H. C. Kwon, S. H. Park, S. I. Woo, *J. Mater. Chem. A* **2013**, *1*, 3694.
[26] C. H. Choi, S. H. Park, S. I. Woo, *ACS Nano* **2012**, *6*, 7084.
[27] R. Jasinski, *Nature* **1964**, *201*, 1212.
[28] H. Liang, S. Brüller, R. Dong, J. Zhang, X. Feng, K. Müllen, *Nat. Commun.* **2015**, *6*, 7992.
[29] Y. Han, Y.-G. Wang, W. Chen, R. Xu, L. Zheng, J. Zhang, J. Luo, R.-A. Shen, Y. Zhu, W.-C. Cheong, C. Chen, Q. Peng, D. Wang, Y. Li, *J. Am. Chem. Soc.* **2017**, *139*, 17269.
[30] P. Zhou, L. Jiang, F. Wang, K. Deng, K. Lv, Z. Zhang, *Sci. Adv.* **2017**, *3*, e1601945.
[31] M. Zhang, Y.-G. Wang, W. Chen, J. Dong, L. Zheng, J. Luo, J. Wan, S. Tian, W.-C. Cheong, D. Wang, Y. Li, *J. Am. Chem. Soc.* **2017**, *139*, 10976.
[32] W. Liu, L. Zhang, X. Liu, X. Liu, X. Yang, S. Miao, W. Wang, A. Wang, T. Zhang, *J. Am. Chem. Soc.* **2017**, *139*, 10790.
[33] W. Liu, Y. Chen, H. Qi, L. Zhang, W. Yan, X. Liu, X. Yang, S. Miao, W. Wang, C. Liu, A. Wang, J. Li, T. Zhang, *Angew. Chem., Int. Ed.* **2018**, *57*, 7071.
[34] H. Wu, H. Li, X. Zhao, Q. Liu, J. Wang, J. Xiao, S. Xie, R. Si, F. Yang, S. Miao, X. Guo, G. Wang, X. Bao, *Energy Environ. Sci.* **2016**, *9*, 3736.
[35] X. Li, W. Bi, M. Chen, Y. Sun, H. Ju, W. Yan, J. Zhu, X. Wu, W. Chu, C. Wu, C. Wu, Y. Xie, *J. Am. Chem. Soc.* **2017**, *139*, 14889.
[36] Y. Qu, Z. Li, W. Chen, Y. Lin, T. Yuan, Z. Yang, C. Zhao, J. Wang, C. Zhao, X. Wang, F. Zhou, Z. Zhuang, Y. Wu, Y. Li, *Nat. Catal.* **2018**, *1*, 781.
[37] D. Deng, X. Chen, L. Yu, X. Wu, Q. Liu, Y. Liu, H. Yang, H. Tian, Y. Hu, P. Du, Y. Hu, P. Du, R. Si, J. Wang, X. Cui, H. Li, J. Xiao, T. Xu, J. Deng, F. Yang, P. N. Duchesne, P. Zhang, J. Zhou, L. Sun, J. Li, X. Pan, X. Bao, *Sci. Adv.* **2015**, *1*, e1500462.
[38] X. Cui, J. Xiao, Y. Wu, P. Du, R. Si, H. Yang, H. Tian, J. Li, W.-H. Zhang, D. Deng, X. Bao, *Angew. Chem., Int. Ed.* **2016**, *55*, 6708.
[39] H. Fei, J. Dong, M. J. Arellano-Jiménez, G. Ye, D. Kim, E. L. G. Samuel, Z. Peng, Z. Zhu, F. Qin, J. Bao, M. J. Yacaman, P. M. Ajayan, D. Chen, J. M. Tour, *Nat. Commun.* **2015**, *6*, 8668.
[40] C. Zhang, J. Sha, H. Fei, M. Liu, S. Yazdi, J. Zhang, Q. Zhong, X. Zou, N. Zhao, H. Yu, Z. Jiang, E. Ringe, B. I. Yakobson, J. Dong, D. Chen, J. M. Tour, *ACS Nano* **2017**, *11*, 6930.
[41] C. Zhang, S. Yang, J. Wu, M. Liu, S. Yazdi, M. Ren, J. Sha, J. Zhong, K. Nie, A. S. Jalilov, Z. Li, H. Li, B. I. Yakobson, Q. Wu, E. Ringe, H. Xu, P. M. Ajayan, J. M. Tour, *Adv. Energy Mater.* **2018**, *8*, 1703487.
[42] J. Guan, Z. Duan, F. Zhang, S. D. Kelly, R. Si, M. Dupuis, Q. Huang, J. Chen, C. Tang, C. Li, *Nat. Catal.* **2018**, *1*, 870.
[43] H. Fei, J. Dong, Y. Feng, C. S. Allen, C. Wan, B. Volosskiy, M. Li, Z. Zhao, Y. Wang, H. Sun, P. An, W. Chen, Z. Guo, C. Lee, D. Chen, I. Shakir, M. Liu, T. Hu, Y. Li, A. I. Kirkland, X. Duan, Y. Huang, *Nat. Catal.* **2018**, *1*, 63.
[44] X. Chen, L. Yu, S. Wang, D. Deng, X. Bao, *Nano Energy* **2017**, *32*, 353.
[45] L. Yang, D. Cheng, X. Zeng, X. Wan, J. Shui, Z. Xiang, D. Cao, *Proc. Natl. Acad. Sci. USA* **2018**, *115*, 6626.
[46] H. T. Chung, D. A. Cullen, D. Higgins, B. T. Sneed, E. F. Holby, K. L. More, P. Zelenay, *Science* **2017**, *357*, 479.
[47] a) S. I. Seneviratne, M. G. Donat, A. J. Pitman, R. Knutti, R. L. Wilby, *Nature* **2016**, *529*, 477; b) S. Wang, X. Li, H. Wu, Z. Tian, Q. Xin, G. He, D. Peng, S. Chen, Y. Yin, Z. Jiang, M. D. Guiver, *Energy Environ. Sci.* **2016**, *9*, 1863; c) X. Wang, Z. Li, J. Shi, H. Wu, Z. Jiang, W. Zhang, X. Song, Q. Ai, *ACS Catal.* **2014**, *4*, 962; d) L. Tang, S. Zhang, Q. Wu, X. Wang, H. Wu, Z. Jiang, *J. Mater. Chem. A* **2018**, *6*, 2964; e) W. Cui, G. Zhang, T. Hu, X. Bu, *Coord. Chem. Rev.* **2019**, *387*, 79; f) S. Zhang, Q. Wu, L. Tang, Y. Hu, M. Wang, J. Zhao, M. Li, J. Han, X. Liu, H. Wang, *ACS Appl. Mater. Interfaces* **2018**, *10*, 39757.
[48] H. B. Yang, S. Hung, S. Liu, K. Yuan, S. Miao, L. Zhang, X. Huang, H. Wang, W. Cai, R. Chen, J. Gao, X. Yang, W. Chen, Y. Huang, H. M. Chen, C. M. Li, T. Zhang, B. Liu, *Nat. Energy* **2018**, *3*, 140.
[49] K. Jiang, S. Siahrostami, T. Zheng, Y. Hu, S. Hwang, E. Stavitski, Y. Peng, J. Dynes, M. Gangisetty, D. Su, K. Attenkofer, H. Wang, *Energy Environ. Sci.* **2018**, *11*, 893.
[50] K. Jiang, S. Siahrostami, A. J. Akey, Y. Li, Z. Lu, J. Lattimer, Y. Hu, C. Stokes, M. Gangishetty, G. Chen, Y. Zhou, W. Hill, W. Cai, D. Bell, K. Chan, J. K. Nørskov, Y. Cui, H. Wang, *Chem* **2017**, *3*, 950.
[51] a) P. Schwach, X. Pan, X. Bao, *Chem. Rev.* **2017**, *117*, 8497; b) Z. Liang, T. Li, M. Kim, A. Asthagiri, J. F. Weaver, *Science* **2017**, *356*, 299.
[52] X. Cui, H. Li, Y. Wang, Y. Hu, L. Hua, H. Li, X. Han, Q. Liu, F. Yang, L. He, X. Chen, Q. Li, J. Xiao, D. Deng, X. Bao, *Chem* **2018**, *4*, 1902.
[53] X. Zhang, J. Guo, P. Guan, C. Liu, H. Huang, F. Xue, X. Dong, S. J. Pennycook, M. F. Chisholm, *Nat. Commun.* **2013**, *4*, 1924.
[54] H.-J. Qiu, Y. Ito, W. Cong, Y. Tan, P. Liu, A. Hirata, T. Fujita, Z. Tang, M. Chen, *Angew. Chem., Int. Ed.* **2015**, *54*, 14031.
[55] L. Zhang, Y. Jia, G. Gao, X. Yan, N. Chen, J. Chen, M. T. Soo, B. Wood, D. Yang, A. Du, X. Yao, *Chem* **2018**, *4*, 1.
[56] a) J. Zhang, T. Wang, P. Liu, S. Liu, R. Dong, X. Zhuang, M. Chen, X. Feng, *Energy Environ. Sci.* **2016**, *9*, 2789; b) P. Abbasi, M. Asadi, C. Liu, S. Sharifi-Asl, B. Sayahpour, A. Behranginia, P. Zapol, R. Shahbazian-Yassar, L. A. Curtiss, A. Salehi-Khojin, *ACS Nano* **2017**, *11*, 453; c) G. Liu, A. W. Robertson, M. M.-J. Li, W. C. H. Kuo, M. T. Darby, M. H. Muhieddine, Y.-C. Lin, K. Suenaga, M. Stamatakis, J. H. Warner, S. Chi, E. Tsang, *Nat. Chem.* **2017**, *9*, 810; d) H. Li, L. Wang, Y. Dai, Z. Pu, Z. Lao, Y. Chen, M. Wang, X. Zheng, J. Zhu, W. Zhang, R. Si, C. Ma, J. Zeng, *Nat. Nanotechnol.* **2018**, *13*, 411.
[57] J. Deng, H. Li, J. Xiao, Y. Tu, D. Deng, H. Yang, H. Tian, J. Li, P. Ren, X. Bao, *Energy Environ. Sci.* **2015**, *8*, 1594.
[58] J. Deng, H. Li, S. Wang, D. Ding, M. Chen, C. Liu, Z. Tian, K. S. Novoselov, C. Ma, D. Deng, X. Bao, *Nat. Commun.* **2017**, *8*, 14430.
[59] Y. Shi, Y. Zhou, D. Yang, W. Xu, C. Wang, F. Wang, J. Xu, X. Xia, H. Chen, *J. Am. Chem. Soc.* **2017**, *139*, 15479.
[60] W. Wu, C. Niu, C. Wei, Y. Jia, C. Li, Q. Xu, *Angew. Chem., Int. Ed.* **2019**, *58*, 2029.

[61] S. Yang, Y. Gong, P. Manchanda, Y. Zhang, G. Ye, S. Chen, L. Song, S. T. Pantelides, P. M. Ajayan, M. F. Chisholm, W. Zhou, *Adv. Mater.* **2018**, *30*, 1803477.
[62] P. Liu, J. Zhu, J. Zhang, P. Xi, K. Tao, D. Gao, D. Xue, *ACS Energy Lett.* **2017**, *2*, 745.
[63] J. Xie, J. Zhang, S. Li, F. Grote, X. Zhang, H. Zhang, R. Wang, Y. Lei, B. Pan, Y. Xie, *J. Am. Chem. Soc.* **2013**, *135*, 17881.
[64] W. Xiao, P. Liu, J. Zhang, W. Song, Y. P. Feng, D. Gao, J. Ding, *Adv. Energy Mater.* **2017**, *7*, 1602086.
[65] a) S. W. Cao, J. X. Low, J. G. Yu, M. Jaroniec, *Adv. Mater.* **2015**, *27*, 2150; b) Z. Tong, D. Yang, Z. Li, Y. Nan, F. Ding, Y. Shen, Z. Jiang, *ACS Nano* **2017**, *11*, 1103; c) Z. Chen, E. Vorobyeva, S. Mitchell, E. Fako, M. A. Ortuño, N. López, S. M. Collins, P. A. Midgley, S. Richard, G. Vilé, J. Pérez-Ramírez, *Nat. Nanotechnol.* **2018**, *13*, 702.
[66] a) W. Ong, L. Tan, Y. H. Ng, S. Yong, S. Chai, *Chem. Rev.* **2016**, *116*, 7159; b) Z. Zhou, Y. Zhang, Y. Shen, S. Liu, Y. Zhang, *Chem. Soc. Rev.* **2018**, *47*, 2298.
[67] X. Li, W. Bi, L. Zhang, S. Tao, W. Chu, Q. Zhang, Y. Luo, C. Wu, Y. Xie, *Adv. Mater.* **2016**, *28*, 2427.
[68] Y. Li, Z. Wang, T. Xia, H. Ju, K. Zhang, R. Long, Q. Xu, C. Wang, L. Song, J. Zhu, J. Jiang, Y. Xiong, *Adv. Mater.* **2016**, *28*, 6959.
[69] a) Y. Cao, S. Chen, Q. Luo, H. Yan, Y. Lin, W. Liu, L. Cao, J. Lu, J. Yang, T. Yao, S. Wei, *Angew. Chem., Int. Ed.* **2017**, *56*, 12191; b) W. Liu, L. Cao, W. Cheng, Y. Cao, X. Liu, W. Zhang, X. Mou, L. Jin, X. Zheng, W. Che, Q. Liu, T. Yao, S. Wei, *Angew. Chem., Int. Ed.* **2017**, *56*, 9312.
[70] Y. Zhao, J. Wan, H. Yao, L. Zhang, K. Lin, L. Wang, N. Yang, D. Liu, L. Song, J. Zhu, L. Gu, L. Liu, H. Zhao, Y. Li, D. Wang, *Nat. Chem.* **2018**, *10*, 924.
[71] J. Zhang, Y. Zhao, X. Guo, C. Chen, C. Dong, R. Liu, C. Han, Y. Li, Y. Gogotsi, G. Wang, *Nat. Catal.* **2018**, *1*, 985.
[72] P. Liu, Y. Zhao, R. Qin, S. Mo, G. Chen, L. Gu, D. M. Chevrier, P. Zhang, Q. Guo, D. Zang, B. Wu, G. Fu, N. Zheng, *Science* **2016**, *352*, 797.
[73] J. Wan, W. Chen, C. Jia, L. Zheng, J. Dong, X. Zheng, Y. Wang, W. Yan, C. Chen, Q. Peng, D. Wang, Y. Li, *Adv. Mater.* **2018**, *30*, 1705369.
[74] a) A. Balanta, C. Godard, C. Claver, *Chem. Soc. Rev.* **2011**, *40*, 4973; b) B. H. Wu, Y. J. Kuang, X. H. Zhang, J. H. Chen, *Nano Today* **2011**, *6*, 75; c) N. Tian, Z. Y. Zhou, S. G. Sun, Y. Ding, Z. L. Wang, *Science* **2007**, *316*, 732; d) S. Linic, U. Aslam, C. Boerigter, M. Morabito, *Nat. Mater.* **2015**, *14*, 567; e) K. Tedsree, T. Li, S. Jones, C. Wong, A. Chan, K. M. K. Yu, P. A. J. Bagot, E. A. Marquis, G. D. W. Smith, S. C. E. Tsang, *Nat. Nanotechnol.* **2011**, *6*, 302.
[75] a) Y. Y. Liang, Y. G. Li, H. L. Wang, J. G. Zhou, J. Wang, T. Regier, H. J. Dai, *Nat. Mater.* **2011**, *10*, 780; b) X. W. Xie, Y. Li, Z. Q. Liu, M. Haruta, W. J. Shen, *Nature* **2009**, *458*, 746.
[76] a) D. H. Deng, L. Yu, X. Q. Chen, G. X. Wang, L. Jin, X. L. Pan, J. Deng, G. Q. Sun, X. H. Bao, *Angew. Chem., Int. Ed.* **2013**, *52*, 371; b) X. Q. Chen, J. P. Xiao, J. Wang, D. H. Deng, Y. F. Hu, J. G. Zhou, L. Yu, T. Heine, X. L. Pan, X. H. Bao, *Chem. Sci.* **2015**, *6*, 3262; c) J. Mahmood, M. A. R. Anjum, J. B. Baek, *Adv. Mater.* **2019**, *31*, 1805062; d) S. J. Kim, J. Mahmood, C. Kim, G. F. Han, S. W. Kim, S. M. Jung, G. Zhu, J. J. D. Yoreo, G. Kim, J. B. Baek, *J. Am. Chem. Soc.* **2018**, *140*, 1737; e) Y. Zhang, N. Wang, N. Jia, J. Wang, J. Sun, F. Shi, Z. Liu, R. Jiang, *Adv. Mater. Interfaces* **2019**, *6*, 1900273.
[77] Y. Y. Liu, H. L. Jiang, Y. H. Zhu, X. L. Yang, C. Z. Li, *J. Mater. Chem. A* **2016**, *4*, 1694.
[78] Y. Hu, J. O. Jensen, W. Zhang, L. N. Cleemann, W. Xing, N. J. Bjerrum, Q. F. Li, *Angew. Chem., Int. Ed.* **2014**, *53*, 3675.
[79] J. Deng, P. Ren, D. Deng, L. Yu, F. Yang, X. Bao, *Energy Environ. Sci.* **2014**, *7*, 1919.
[80] J. Deng, P. Ren, D. Deng, X. Bao, *Angew. Chem., Int. Ed.* **2015**, *54*, 2100.
[81] M. Tavakkoli, T. Kallio, O. Reynaud, A. G. Nasibulin, C. Johans, J. Sainio, H. Jiang, E. I. Kauppinen, K. Laasonen, *Angew. Chem., Int. Ed.* **2015**, *54*, 4535.
[82] D. Y. Chung, S. W. Jun, G. Yoon, H. Kim, J. M. Yoo, K. Lee, T. Kim, H. Shin, A. K. Sinha, S. G. Kwon, K. Kang, T. Hyeon, Y. Sung, *J. Am. Chem. Soc.* **2017**, *139*, 6669.
[83] X. Cui, P. Ren, D. Deng, J. Deng, X. Bao, *Energy Environ. Sci.* **2016**, *9*, 123.
[84] Y. Zhao, J. Zhang, K. Li, Z. Ao, C. Wang, H. Liu, K. Sun, G. Wang, *J. Mater. Chem. A* **2016**, *4*, 12818.
[85] B. Xia, Y. Yan, N. Li, H. Wu, X. Lou, X. Wang, *Nat. Energy* **2016**, *1*, 15006.
[86] Y. Tu, P. Ren, D. Deng, X. Bao, *Nano Energy* **2018**, *52*, 494.
[87] a) L. Ferrighi, M. Datteo, G. Fazio, C. D. Valentin, *J. Am. Chem. Soc.* **2016**, *138*, 7365; b) C. Riedl, C. Coletti, T. Iwasaki, A. A. Zakharov, U. Starke, *Phys. Rev. Lett.* **2009**, *103*, 246804; c) Y. Yao, Q. Fu, Y. Y. Zhang, X. Weng, H. Li, M. Chen, L. Jin, A. Dong, R. Mu, P. Jiang, L. Liu, H. Bluhm, Z. Liu, S. B. Zhang, X. Bao, *Proc. Natl. Acad. Sci. USA* **2014**, *111*, 17023; d) Y. Zhang, X. Weng, H. Li, H. Li, M. Wei, J. Xiao, Z. Liu, M. Chen, Q. Fu, X. Bao, *Nano Lett.* **2015**, *15*, 3616; e) P. Sutter, J. T. Sadowski, E. Sutter, *Phys. Rev. B* **2009**, *80*, 245411.
[88] L. Gao, Y. Wang, H. Li, Q. Li, N. Ta, L. Zhuang, Q. Fu, X. Bao, *Chem. Sci.* **2017**, *8*, 5728.
[89] Y. Zhou, W. Chen, P. Cui, J. Zeng, Z. Lin, E. Kaxiras, Z. Zhang, *Nano Lett.* **2016**, *16*, 6058.
[90] H. Li, J. Xiao, Q. Fu, X. Bao, *Proc. Natl. Acad. Sci. USA* **2017**, *114*, 5930.
[91] Q. Fu, X. Bao, *Chem. Soc. Rev.* **2017**, *46*, 1842.